Supporting information for

Title: Yeast homologous recombination-based promoter engineering for the activation of silent natural product biosynthetic gene clusters

Authors: Daniel Montiel[*], Hahk-Soo Kang[*], Fang-Yuan Chang, Zachary Charlop-Powers and Sean F. Brady[1]

Author affiliation: Laboratory of Genetically Encoded Small Molecules, The Rockefeller University, 1230 York Avenue, New York, NY 10065.

[*]Montiel, D. and Kang, H.-S. contributed equally to this work

[1]**Corresponding Author:** Sean F. Brady

Contact Information: Laboratory of Genetically Encoded Small Molecules
The Rockefeller University
1230 York Avenue
New York, NY 10065
Phone: 212-327-8280
Fax: 212-327-8281
Email: sbrady@rockefeller.edu

SI methods.

Yeast strain, plasmids and primers *S. cerevisiae* BY4727 (genotype MATα his3Δ200::leu2Δ0::lys2Δ0::met15Δ0::trp1Δ63::ura3Δ0) was purchased from ATCC (ATCC No. 200889). Plasmids pRS401, pRS403, pRS404, pRS405 and pR317, which contain the marker genes MET15, HIS3, TRP1, LEU2 and LYS2, respectively, were obtained from the Cross Lab at the Rockefeller University. Plasmid pFA6-KanMX6 containing the KanMX selectable marker was purchased from Addgene (Plasmid No. 39296). Amino acid SC dropout media was purchased from Sunrise Science Products in San Diego, CA. Primers were synthesized by Eurofins MWG Operon.

Clone retrofitting: To permit promoter engineering in yeast and heterologous expression in model Actinomycetes hosts, all clones carrying gene clusters were retrofitted with the 8.7 kb *SspI* fragment from pTARa (1), which contains yeast elements including a CEN/ARS (single copy number yeast origin of replication), a yeast selectable marker URA3, and *Streptomyces* elements including an origin of transfer, a ΦC31 integrase and an apramycin resistance gene. Cosmids AR1455 (Reb gene cluster) and AR60 (Tam gene cluster) were digested with *Psi*I, which due to an AT-rich recognition site does not cut often within cloned biosynthetic gene clusters derived from GC-rich genomes like those of Actinobacteria. *Psi*I digested cosmid and *SspI* digested pTARa were column (QIAprep Spin Column, QIAGEN) purified and ligated directly without gel purification. Retrofitted cosmids were identified by selection on chloramphenicol and apramycin.

TAR assembly: The two overlapping eDNA cosmid clones (AZ25-292 and AZ25-153) predicted to contain the Lzr gene cluster were assembled into a large insert bacterial artificial chromosome (BAC) clone in yeast using TAR. A pathway-specific Lzr TAR capture vector was constructed using a two-step PCR process described previously (2). The primers used for construction of the TAR capture vector are listed in Table S6. For TAR assembly, 300 ng of each DraI-cut cosmid (AZ25-292 and AZ25-153) were mixed with 200 ng of the HpaI-digested pathway-specific capture vector and then transformed into 200 *μ*l of *Saccharomyces cerevisiae* CRY1-2 spheroplasts prepared according to published protocols (2). Transformed spheroplasts were mixed with SC dropout top agar (1 M sorbitol, 1.92 g/L synthetic complete uracil dropout supplement, 6.7 g/L yeast nitrogen base, 2% glucose and 2.5% agar) and overlaid onto SC dropout plates without uracil. Plates were incubated at 30 °C for approximately 72 hours, until colonies appeared. Twelve yeast colonies were picked and cultured overnight in SC dropout liquid media without uracil. DNA was isolated using a modified zymolyase lysis protocol (3) and screened by PCR with primers designed to recognize sequences from each cosmid. BAC clones that amplified with all primer sets were electroporated into *E. coli* EPI300 (Epicentre). DNA miniprepped from these *E. coli* EPI300 cells was PGM-sequenced to confirm the correct reassembly of the two overlapping cosmids into the predicted BAC clone (BAC-AZ25-292/153).

BY4727 *Δdnl4* strain construction. A knock-out of DNL4, the gene that encodes the DNA ligase required for NHEJ was constructed using a PCR amplicon-based gene deletion strategy (Figure S2) (4). Briefly, the deletion cassette was constructed by PCR-amplification of the KanMX module from the plasmid pFA6-kanMX4 using a primer set containing 40 bp sequences homologous to the upstream and downstream regions of the DNL4 gene (Table S2). Approximately 1 μg of the column-purified PCR product was transformed into BY4727 and plated on a YPD agar plate containing G418 (200 μg/ml). Colonies were picked after three days and the deletion of the DNL4 gene was confirmed by PCR-based genotyping using primer sets that generate amplicons bridging the yeast chromosome and the inserted KanMX cassette.

Simultaneous exchange of multiple promoter cassettes. Each promoter cassette was first inserted into a gene cluster in parallel using 40 bp homology arms. As we were unable to find robust promoter/operon prediction software for natural product gene clusters, we manually assigned operon structures based on two criteria: directionality of genes and spacing between ORFs. Promoter cassettes containing 500 bp homology arms were generated by PCR using these constructs as templates. Promoter cassettes with longer homology arms could also be obtained using overlap extension PCR; however, we have found that this method often requires extensive PCR optimization to obtain sufficient clean PCR product for yeast recombination experiments. PCR products were confirmed by gel analysis, column-purified to yield a final amplicon concentration of 300 – 400 ng/μl. Four micrograms of a gene cluster were co-transformed with 2 μg of each promoter cassette into the BY4727 *Δdnl4* strain using the LiAc/ss carrier DNA/PEG yeast transformation protocol outlined in the manuscript. Transformants were selected on the appropriate multiple amino acid SC dropout agar plate.

PCR-based genotyping. The correct insertion of promoter cassettes was verified by PCR-based genotyping using primer sets (Tables S3-S6) that generated PCR amplicons bridging the newly inserted promoter cassettes and the target gene clusters. Colonies were picked from the appropriate amino acid SC dropout agar plates, inoculated into 3 ml of an appropriate liquid SC dropout media and grown overnight. Overnight cultures were harvested by centrifugation (3,200xg, 10 min) and a yeast DNA mini-prep was performed using a modified zymolyase lysis protocol (3). Yeast mini-prepped DNA was analyzed by PCR using primer sets that generated amplicons bridging the gene cluster and the inserted promoter cassette. PCR positive yeast mini-prepped DNA was electroporated into *E. coli* EC100 (Epicentre). *E. coli* colonies were re-analyzed using the same primer sets and the resulting amplicons were sequenced to ensure that no mutations occurred during the recombination process.

Replacement of *LzrX1* Gene. The *lzrX1* pseudogene was replaced with the *abeX1* gene from the BE-54017 gene cluster using the approach outlined in Figure S6. The *abeX1* gene was initially amplified from the BE-54017 gene cluster using a C-terminal specific primer with a 40 bp Lzr gene cluster specific homology arm and an N-terminal specific primer with a Lys2 cassette specific extension. At the same time, the Lys2 cassette was amplified using a primer with a 40 bp Lzr gene cluster specific homology arm and a primer with an *abeX1* specific extension. Primers sequences are listed in Table S6. These amplicons were gel purified and 100 ng of each amplicon was used as template in a second round PCR reaction with the primers containing Lzr gene cluster homology arms. After gel purification, 4 μg of amplicon was transformed, using the LiAc/ss carrier DNA/PEG method, into a yeast strain containing the Lzr gene cluster with the first two promoter sites already replaced (Figure 3). Yeast colonies were genotyped as described above and DNA from PCR positive colonies was electroporated into *E. coli* EPI300 to yield the re-engineered Lzr gene cluster.

Heterologous expression, HPLC analysis and compound isolation: Correctly re-engineered gene clusters were transformed into *E. coli* S17.1 and then transferred into *S. albus* via intergeneric conjugation. *S. albus* cultures harboring the refactored Reb and Tam gene clusters were grown in R5A media (2 X 50 mL) for 7 days at 30 °C (200 rpm). Cultures were extracted with 1/3 volume of ethyl acetate. The extracts were dried and resuspended in 500 μL of methanol. The presence of rebeccamycin (**1**) or tetarimycin A (**2**) in extracts was confirmed by HPLC and LC-MS analysis using a reversed phase C_{18} analytical column (4.6 X 150 mm) and a gradient from 5% to 100% acetonitrile in water over 30 min. Lazarimides A (**7**), B (**6**) and C (**5**) were isolated from the cultures of *S. albus* harboring the refactored Lzr gene clusters using the following protocol. TSB seed cultures were grown overnight at 30 °C (200 rpm). Twenty four milliliters of seed culture was used to inoculate 6 L of R5A media. After 14 days (30 °C, 200 rpm), the entire culture was extracted with 2 volumes of ethyl acetate. The crude extract was partitioned using a modified Kupchan scheme (5). The dichloromethane fraction was dried down, resuspended in methanol and then partitioned by silica gel flash chromatography (hexane:ethyl acetate gradient, 100:0 to 0:100 over 50 minutes). Compounds were further purified using two rounds of isocratic reversed-phase HPLC (55:45 water:acetonitrile and 35:65 water:methanol) to yield pure compounds **5** - **7**. From 6L of culture, we isolated 2.3 mg of **7**, 1.8 mg of **6** and 3.1 mg of **5**. Analytical LCMS data was collected on a Micromass ZQ instrument (Waters). HRESIMS was performed on an LCT Premier XE mass spectrometer (Waters) at Memorial Sloan Kettering Cancer Center Analytical Core Facility in negative ion mode.

Antiproliferative assay. The antiproliferative activity of lazarimides A (**7**), B (**6**) and C (**5**) was evaluated in triplicate using the colon carcinoma cell line HCT-116 (ATCC; CCL-247) (6). For assays, frozen HCT-116 cells were thawed and grown in McCoy's 5A Modified Medium (Gibco) supplemented with 10% (v/v) FBS. Cells were sub-cultured once, and then cells in log phase growth were harvested by trypsinization. Trypsinized cells were seeded into 96-well plates (1,000 cells/well) and incubated overnight at 37 °C in the presence of 5% CO_2. Compounds **5** – **7** (10 mg/ml in DMSO) were sequentially diluted in culture media (2-fold dilution starting at 50 μg/ml) across a 96-well plate and 100 μL was transferred to the appropriate well in an assay plate. The plates were incubated at 37 °C for 3 days and then evaluated for viability using a crystal violet-based colorimetric assay (7). Cell viability was recorded based on the absorbance at 590 nm in compound treated well relative to DMSO control wells.

SI discussions.

Transcriptional interference test. The convergent transcription of two neighboring strong promoters has been observed in some instances to cause premature transcriptional termination and silencing due to the collision of elongation complexes (8). To investigate whether this phenomenon might interfere with molecule production using our promoter cassettes, we inserted the MET15 bi-directional promoter cassette in front of *rebR* (Figure S3biii; Figure S4). HPLC analysis of organic extracts derived from a culture of *S. albus* transformed with this construct showed no significant differences in rebeccamycin production when compared to extracts derived from the wild-type Reb gene cluster or the Reb gene cluster re-engineered with the MET15 unidirectional promoter (Figure S3bii), suggesting that at least in this model system convergent transcription between our synthetic promoters does not profoundly affect the level of molecule production from the re-engineered gene cluster. Although additional studies are needed to make a more general conclusion, these results taken together with similar observations from promoter engineering experiments with Tam gene cluster suggest that our promoter replacement cassettes will not generically cause silencing of nearby operons.

Structure determination of lazarimides A – C. The structures of lazarimides A (**7**), B (**6**) and C (**5**) were determined using 1D and 2D NMR and HRESIMS data.

Lazarimide A (7): Lazarimide A (**7**) was isolated from the extract of *S. albus* harboring the re-engineered Lzr gene cluster with four promoter cassettes (P1 – P4) and the *abeX1* oxidative gene. A pseudo molecular ion observed at *m/z* 486.0260 ([M-H]$^-$) in the HRESIMS spectrum suggested the molecular formula of **7** as $C_{22}H_{15}Cl_2N_3O_6$. The HRESIMS spectrum displayed strong M+2 and M+4 signals, suggesting the presence of two chlorines. As expected from bioinformatic analysis, the ^{1}H NMR spectrum of **7** showed signals characteristic for the indolotryptoline family of compounds including a characteristic indole NH (H-13) at 11.59 ppm, an N-Me (H-14) at 2.86 ppm and aromatic signals around 8 ppm (9). Analysis of the COSY and HMBC spectra established two substructures designated as **a** and **b** (Figure S7). COSY correlations between H-1 (δ_H 7.51) and H-2 (δ_H 7.17, ortho coupling, J = 8.6 Hz), and between H-2 and H-4 (δ_H 7.88, meta coupling, J = 1.7 Hz) together with HMBC correlations from H-13 (δ_H 11.59, NH) to C-13a (δ_C 136.6) and C-12b (δ_C 127.9), from H-1 (δ_H 7.51) to C-3 (δ_C 124.7) and C-4a (δ_C 126.0), from H-2 (δ_H 7.17) to C-4 (δ_C 119.4) and C-13a (δ_C 136.6), and from H-4 to C-4a (δ_C 126.0) and C-13a (δ_C 136.6) indicated the presence of an indole moiety with chlorination at C-3 and additional di-substitutions at C-4b and C-12b, which is typically observed in the indolotryptoline family of compounds (9). HMBC correlations from H-14 (δ_H 2.86) to C-5 (δ_C 174.2) and C-7 (δ_C 171.4), from C4c-OH (δ_H 7.16) to C-4b (δ_C 103.8), C-4c (δ_C 74.8), C-7a (δ_C 87.1) and C-5 (δ_C 174.2), and from C7a-OH (δ_H 8.17) to C-4c (δ_C 74.8), C-7a (δ_C 87.1) and C-7 (δ_C 171.4) revealed the structure of an *N*-methyl-dihydroxy succinimide with additional substitutions at C-4c and C-7a. This succinimide moiety was connected to a chlorinated indole moiety via an HMBC correlation from C4c-OH (δ_H 7.16) and H-4 (δ_H 7.88) to C-4b (δ_C 103.8) establishing substructure **a**. Substructure **b** was also defined by HMBC correlations. HMBC correlations from C10-OH (δ_H 9.81) to C-9 (δ_C 118.0), C-10 (δ_C 147.2) and C-11 (δ_C 102.5), from H-8 (δ_H 8.04) to C-10 (δ_H 147.2) and C-11a (δ_C 121.2), from H-11 (δ_H 7.16) to C-7c (δ_C 130.4) and C-9 (δ_C 118.0), and from 12-OMe (δ_H 4.02) and H-11 (δ_H 7.16) to C-12 (δ_C 135.7) indicate that substructure **b** is another indole moiety with chlorination at C-9, hydroxylation at C-10, and methoxylation at C-12 as well as two additional substitutions.

HMBC correlations connecting substructures **a** and **b** were not observed due to the presence of quaternary carbons throughout the structure. However, the presence of the indolotryptoline scaffold could be deduced based on carbon chemical shift comparisons to known indolotryptolines, NOESY correlation data and the bioinformatics analysis of the gene cluster. The downfield-shifted chemical shift of C-7a (δ_C 87.1) compared to that of C4c (δ_C 74.8) suggests that C-7a is nitrogen-substituted. The presence of an indolotryptoline structure was further confirmed by an NOE correlation observed between 12-OMe and H-13 (NH). The NOE correlation observed between C4c-OH and C7a-OH suggested the "*cis*" configuration between these two hydroxyl groups, completing the structure determination of **7**. Based on the X-ray crystal structure of lazarimide C (**5**), the absolute configurations of hydroxyl group-bearing stereogenic carbons C-4c and C-7a in the structure of **7** can be deduced. The X-ray crystallography of **5** assigned the configuration of C-4c as "*S*", and the absolute configuration of this carbon is likely to remain the same during the oxidation-mediated indole ring flipping step (10), thus together with the "*cis*" relationship observed between hydroxyl groups as C-4c and C-7a, the absolute configurations of C-4c and C-7a in the structure of **7** were deduced as "*S"* and *"R*", respectively. This assignment is consistent with the absolute configuration reported for cladoniamide A (9).

Lazarimide B (6): Lazarimide B (**6**) was isolated from the extract of *S. albus* harboring the reengineered Lzr gene cluster with three promoter cassettes (P1 – P3) and the *abeX1* oxidative gene. The molecular ion observed at 470.0320 ($[M-H]^-$) in the HRESIMS spectrum suggested a molecular formula of $C_{22}H_{15}Cl_2N_3O_5$. The HRESIMS spectrum of **6** also showed strong signals corresponding to M+2 and M+4 indicating the presence of two chlorines. The structure of lazarimide B (**6**) was determined by comparison of the NMR spectra with those for **7**. Compound **6** showed nearly identical ^1H and ^{13}C NMR data to those of **7** except for the set of chemical shifts that would be predicted to correspond to the flipped indole ring moiety. In the ^1H proton spectra, differences in both chemical shifts and splitting patterns were observed. First, one additional proton signal was observed, which showed COSY correlations with H-8 (δ_H 8.11, J = 1.8 Hz) and H-11 (δ_H 7.75, J = 8.5 Hz). This together with the fact that compound **6** was obtained without a promoter replacement for the operon containing the P450 hydroxylase gene indicated that compound **6** is the non-hydroxylated analog of **7**.

Lazarimide C (5): The structure of lazarimide C (**5**) was also determined by comparison of the NMR spectra with those of **6**. Compound **5** appears in extracts both with and without a functional *lzrX1* homolog suggesting it is an indolocarbazole, and not an indolotryptoline, based tryptophan dimer. The molecular formula is predicted to be $C_{20}H_{11}Cl_2N_3O_4$ on the basis of the molecular ion signal observed at 426.0056 ($[M-H]^-$) as well as the presence of M+2 and M+4 signals. Two sets of AMX spin systems observed in the ^1H NMR and COSY spectra indicated the presence of two unsymmetrical indole rings in the structure of **5**. No N-Me nor O-Me signals were observed in the ^1H NMR spectrum of **5**. HMBC correlations from H-13 (δ_H 11.54, indole NH) to C-1 (δ_C 113.5) protonated with H-1 (δ_H 7.54, ortho coupling J = 8.6 Hz) and from H-12 (δ_H 11.42, indole NH) to C-11 (δ_H 111.6) protonated with H-11 (δ_H 7.64, meta coupling J = 1.9 Hz) suggested that chlorines are attached to C-3 and C-10. This was further supported by HMBC correlations from C4c-OH (δ_H 6.48) and H-4 (δ_H 7.95, meta coupling J = 1.5 Hz) to C-4b (δ_C 108.7), and from C7a-OH (δ_H 6.48) and H-8 (δ_H 7.96, ortho coupling J = 7.2 Hz), completing the planar structure of **5** (Figure S8). The absolute configurations of the two hydroxyl group-bearing stereogenic carbons, C-4c and C-7b, were assigned by single crystal X-ray crystallography. The X-ray structure of **5** showed that the two hydroxyl groups are in a "*cis*" relationship with the absolute configurations of "*S, R*" (4c, 7a). The "cis" configuration in **5** is consistent with the crystal structure for the corresponding 'unflipped' indolocarbazole intermediate observed in cladoniamide A biosynthesis(11).

X-ray crystallography for lazarimide C (5). Lazarimide C (**5**) was crystalized by slow evaporation from acetone and water. A very small (0.15 x 0.10 x 0.05 mm^3) single crystal was mounted on a Bruker X8 APEX II diffractometer (MoK_α radiation) and cooled to -80 ºC. Data collection and reduction were done using Bruker APEX2 (12) and SAINT+ (13) software packages. An empirical absorption correction was applied with SADABS (14). The data resolution was low due to the smallness of the specimen. The structure was solved by direct methods and refined on F^2 by full matrix least-squares techniques using SHELXTL (15) software package. All non-hydrogen atoms were refined anisotropically. Hydrogen atoms were added in calculated positions. Overall 10725 reflections were collected, 5008 of which were symmetry independent (R_{int} = 0.0506); with 3307 'strong' reflections (with $F_o > 4sF_o$). Final R_1 = 6.5%.

SI References

1. Kim JH*, et al.* (2010) Cloning large natural product gene clusters from the environment: piecing environmental DNA gene clusters back together with TAR. *Biopolymers* 93(9):833-844.
2. Kallifidas D & Brady SF (2012) Reassembly of functionally intact environmental DNA-derived biosynthetic gene clusters. *Methods Enzymol* 517:225-239.
3. Kouprina N & Larionov V (2008) Selective isolation of genomic loci from complex genomes by transformation-associated recombination cloning in the yeast Saccharomyces cerevisiae. *Nat Protoc* 3(3):371-377.
4. Wach A, Brachat A, Pohlmann R, & Philippsen P (1994) New heterologous modules for classical or PCR-based gene disruptions in Saccharomyces cerevisiae. *Yeast* 10(13):1793-1808.
5. Kupchan SM, Britton RW, Ziegler MF, & Sigel CW (1973) Bruceantin, a new potent antileukemic simaroubolide from Brucea antidysenterica. *J Org Chem* 38(1):178-179.
6. Brattain MG, Fine WD, Khaled FM, Thompson J, & Brattain DE (1981) Heterogeneity of malignant cells from a human colonic carcinoma. *Cancer Res* 41(5):1751-1756.
7. Zivadinovic D, Gametchu B, & Watson CS (2005) Membrane estrogen receptor-alpha levels in MCF-7 breast cancer cells predict cAMP and proliferation responses. *Breast Cancer Res* 7(1):R101-112.
8. Shearwin KE, Callen BP, & Egan JB (2005) Transcriptional interference--a crash course. *Trends Genet* 21(6):339-345.
9. Williams DE*, et al.* (2008) Cladoniamides A-G, tryptophan-derived alkaloids produced in culture by *Streptomyces uncialis*. *Org Lett* 10(16):3501-3504.
10. Chang FY & Brady SF (2011) Cloning and characterization of an environmental DNA-derived gene cluster that encodes the biosynthesis of the antitumor substance BE-54017. *J Am Chem Soc* 133(26):9996-9999.
11. Du Y-L, Williams DE, Patrick BO, Andersen RJ, & Ryan KS (2014) Reconstruction of Cladoniamide Biosynthesis Reveals Nonenzymatic Routes to Bisindole Diversity. *ACS Chem Bio* 9(12):2748-2754.
12. APEX2 v.1.0-22 (2004) User Manual, Bruker AXS Inc., Madison WI 53719.
13. SAINT+ v.6.02 (1999) User Manual, Bruker AXS Inc., Madison WI 53719.
14. G.M.Scheldrick (1996) SADABS, Program for Empirical Absorption Correction of Area Detector Data, University of Göttingen.
15. G.M.Scheldrick, (1999) SHELXTL v. 5.10 Bruker AXS Inc., Madison WI 53719.

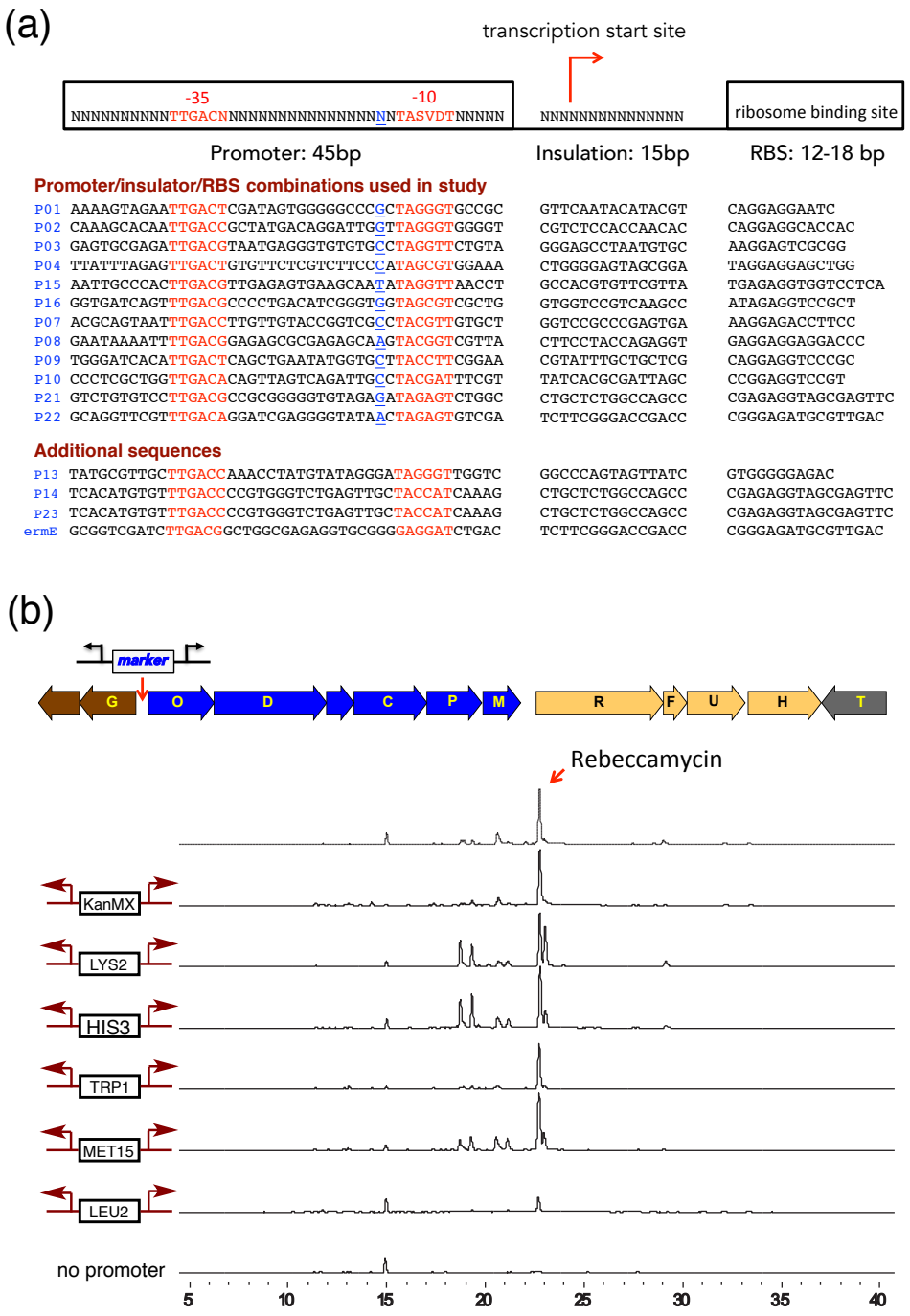

Figure S1. Construction and testing of bi-directional promoter cassettes in yeast homologous recombination reactions. (a) Cartoon illustrating the organization of the promoter/insulator/RBS sequences used to create the bi-directional promoter cassettes. The sequences of promoter/insulator/RBS sequences that successfully induced production of rebeccamycin in promoter exchange experiments using the Reb gene cluster are listed. The twelve sequences used to build the six bi-directional promoter cassettes used in this study are listed, as are the four additional sequences that induced rebeccamycin production. (b) A cartoon of the Reb cluster indicating the location of the promoter cassette insertion site and HPLC chromatograms of *S. albus* extracts harboring Reb gene clusters refactored with the six bi-directional promoter cassettes used for promoter engineering in this study.

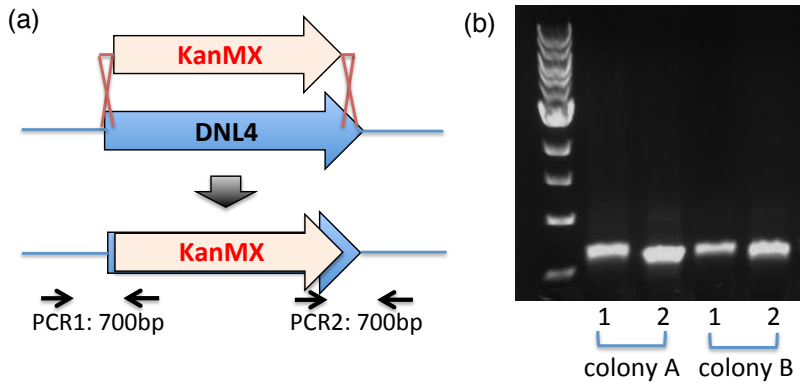

Figure S2. Overview of the deletion of the DNL4 gene in *S. cerevisiae* strain BY4727 to create an NHEJ-deficient strain. (a) Cartoon depicting the PCR-generated gene deletion strategy and locations of PCR-genotyping primers. The DNL4 gene in the BY4727 chromosome was replaced with the KanMX gene. (b) PCR-based genotyping of two yeast colonies with the BY4727 Δ*dnl4* genotype. The correct replacement of the DNL4 gene by the KanMX gene was confirmed using two primer sets designed to generate amplicons (PCR1 and PCR2) that bridges the BY4727 chromosome and the KanMX cassette.

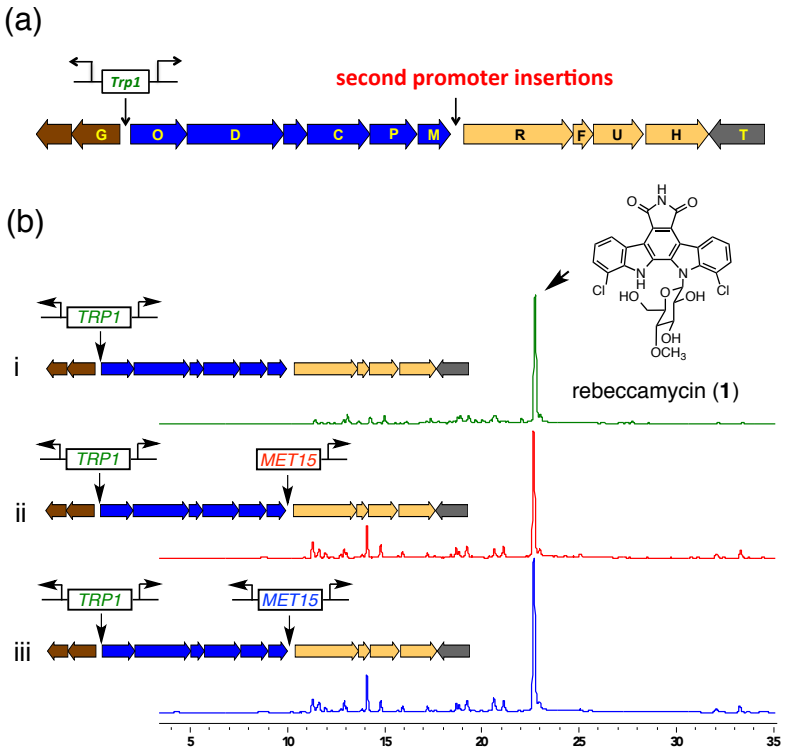

Figure S3. Transcriptional interference test. (a) Cartoon indicating the location of the two promoter sites in the Reb gene cluster used for transcriptional interference testing. (b) HPLC chromatograms of *S. albus* extracts harboring refactored Reb gene clusters containing a TRP1 bi-directional promoter cassette in the first promoter site and either no promoter cassette (bi), a MET15 uni-directional promoter cassette (bii) or a bi-directional promoter cassette (biii) in the second promoter site. The refactored Reb gene cluster with a bi-directional cassette in the second promoter site showed essentially the same level of rebeccamycin production as the refactored Reb gene cluster with no promoter cassette in the second promoter site.

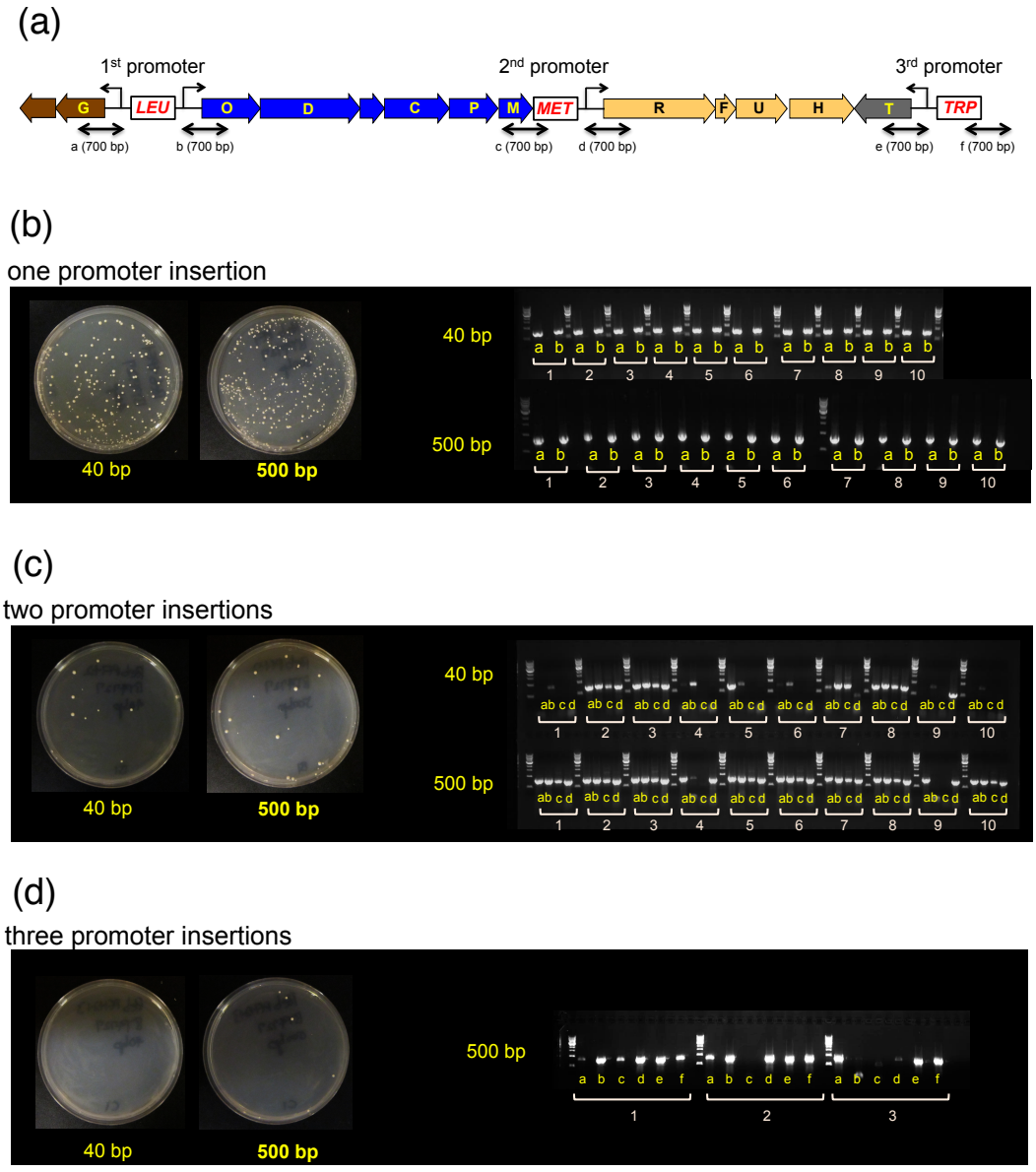

Figure S4. Results of multiplexed promoter cassette insertion experiments for refactoring the Reb gene cluster. (a) Cartoon of the Reb gene cluster indicating the promoter insertion sites and locations of amplicons generated for PCR-genotyping experiments to test for correct promoter insertion. (b)-(d) Pictures of yeast colonies generated from multiplexed promoter cassette insertion experiments along with the gel analysis of the PCR-based genotyping. For the one (a) and two (b) promoter cassette insertions, ten yeast colonies were tested. All three colonies generated in the three-promoter cassette insertion experiment using 500 bp homology arms cassettes were tested.

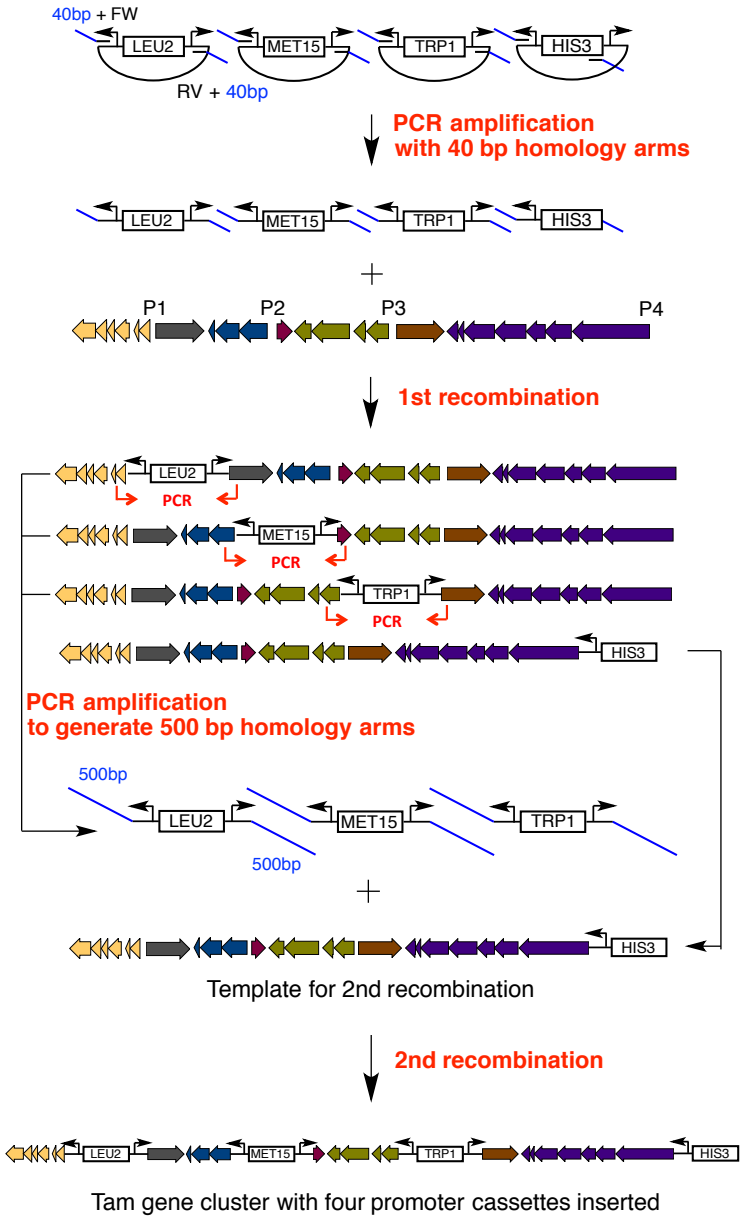

Figure S5. Cartoon overviewing the process of refactoring the four bi-directional promoter sites (P1-P4) in the Tam gene cluster. Initially, the LEU2, MET15, TRP1 and HIS3 bi-directional synthetic promoter cassettes were amplified with pathway-specific 40 bp homology arms. These four bi-directional promoter cassettes were each used to perform a single promoter cassette insertion into the Tam gene cluster. Single promoter cassette insertions were performed in parallel. LEU2, MET15 and TRP1 promoter cassettes were then re-amplified from the single promoter constructs to generate bi-directional promoter cassettes with 500 bp homology arms. The 400 bp cassettes were co-transformed with the Tam gene cluster already containing the HIS3 promoter cassette.

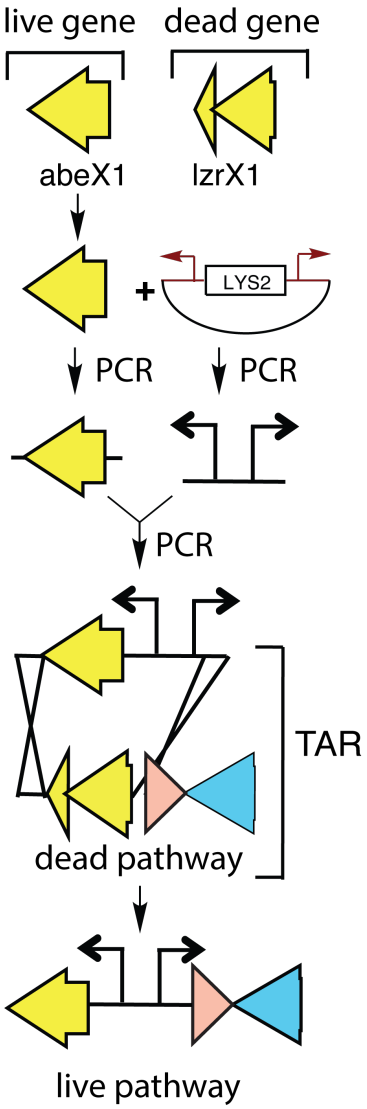

Figure S6. Cartoon of the two-step PCR protocol used to combine the promoter cassette and *abeX1* gene into a single amplicon.

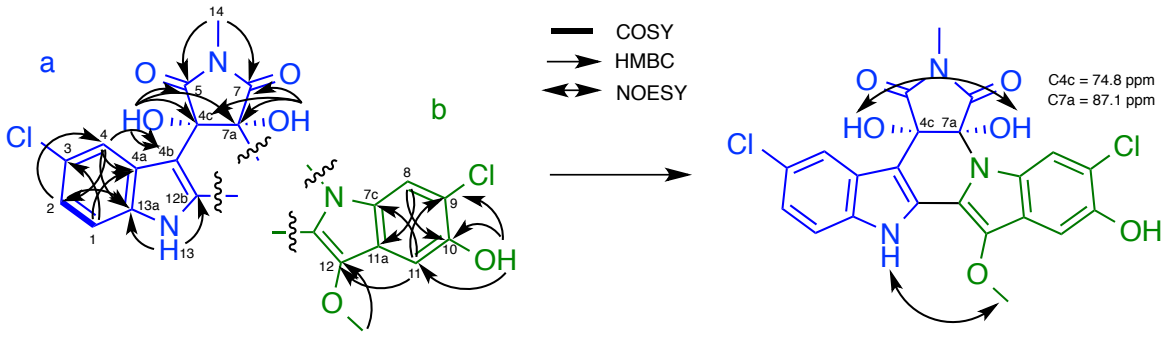

Figure S7. Key 2D NMR correlations used to help define the structure of lazarimide A (**7**). The HMBC correlations for substructure **a** support a halogenated indole moiety joined to a succinimide group. The HMBC correlations for substructure **b** support a halogenated and methoxylated indole ring. A NOESY correlation between the central hydroxyl groups supports the 'cis' configuration shown. A NOESY correlation between the amide proton and methoxy protons is used to support the connection between substructures **a** and **b**.

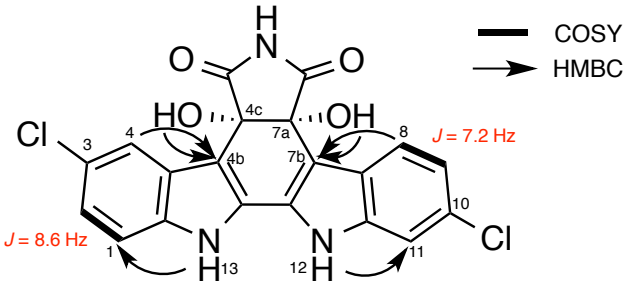

Figure S8. Key NMR data used in the structure determination of lazarimide C (**5**). The presence of two COSY spin systems suggests an asymmetric halogenation pattern for the two indole rings. One of the amide protons shows a HMBC correlation to a carbon attached to one of the COSY spin system protons. An HMBC correlation from one amide proton is seen to carbon bound to proton that is not involved in either of the COSY spin systems. These observations support the depicted halogenation pattern and are also supported by an analogous argument for the HMBC correlations at positions 4 and 8 to the quaternary carbons a 4b and 7b. The NMR structure is consistent with the crystal structure of **5**.

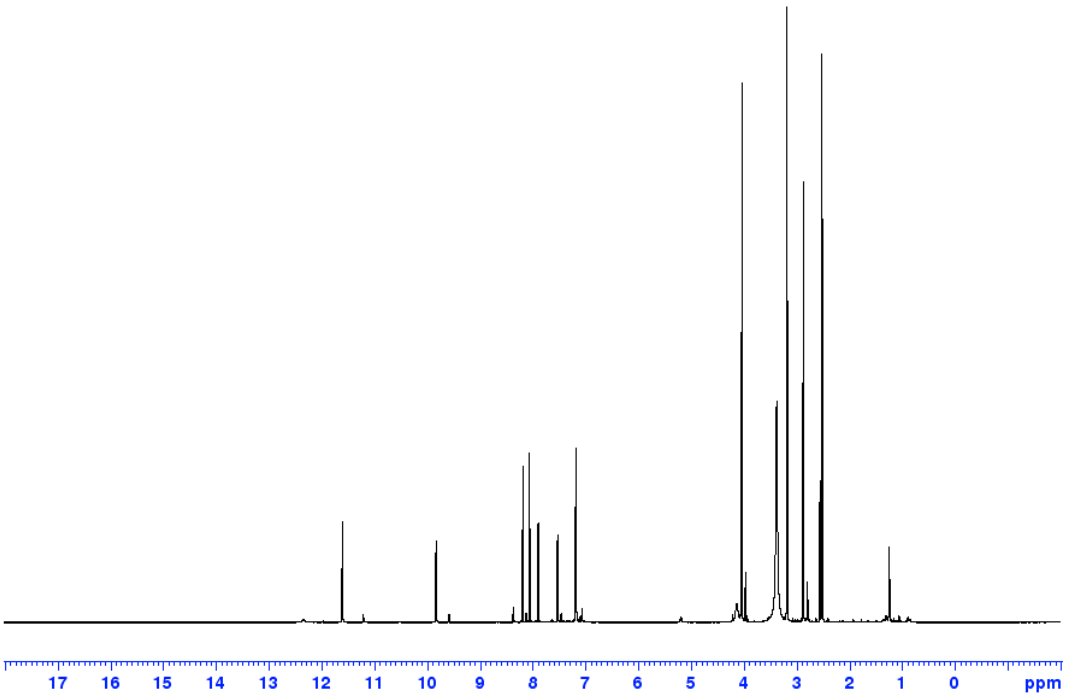

Figure S9. ^{1}H NMR spectrum (DMSO-d_6, 600 MHz) of lazarimide A (**7**).

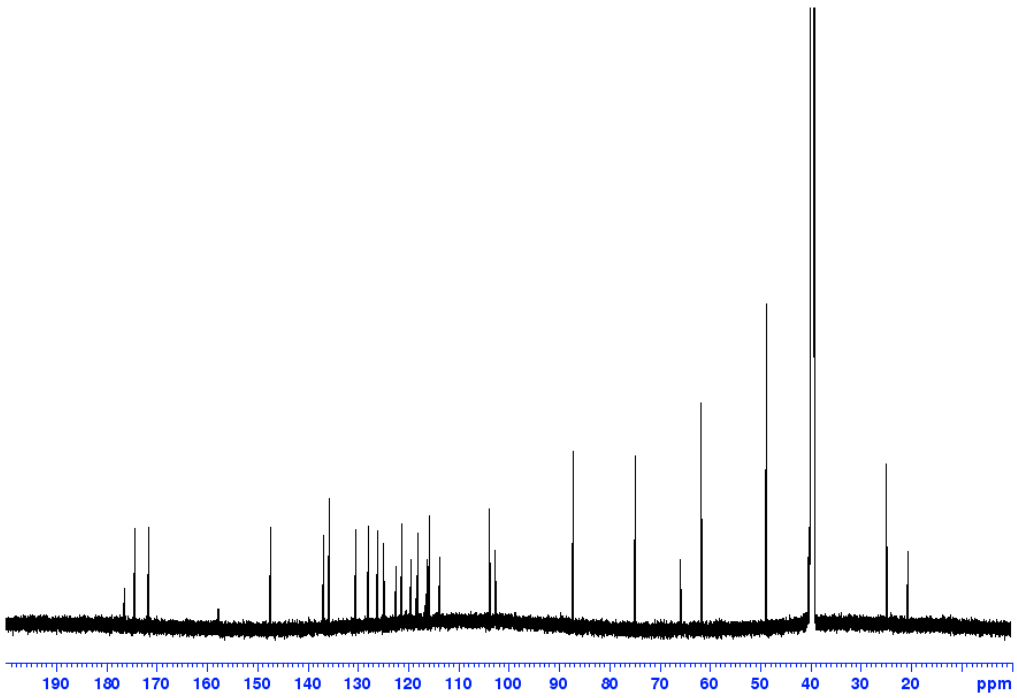

Figure S10. ^{13}C NMR spectrum (DMSO-d_6, 150 MHz) of lazarimide A (**7**).

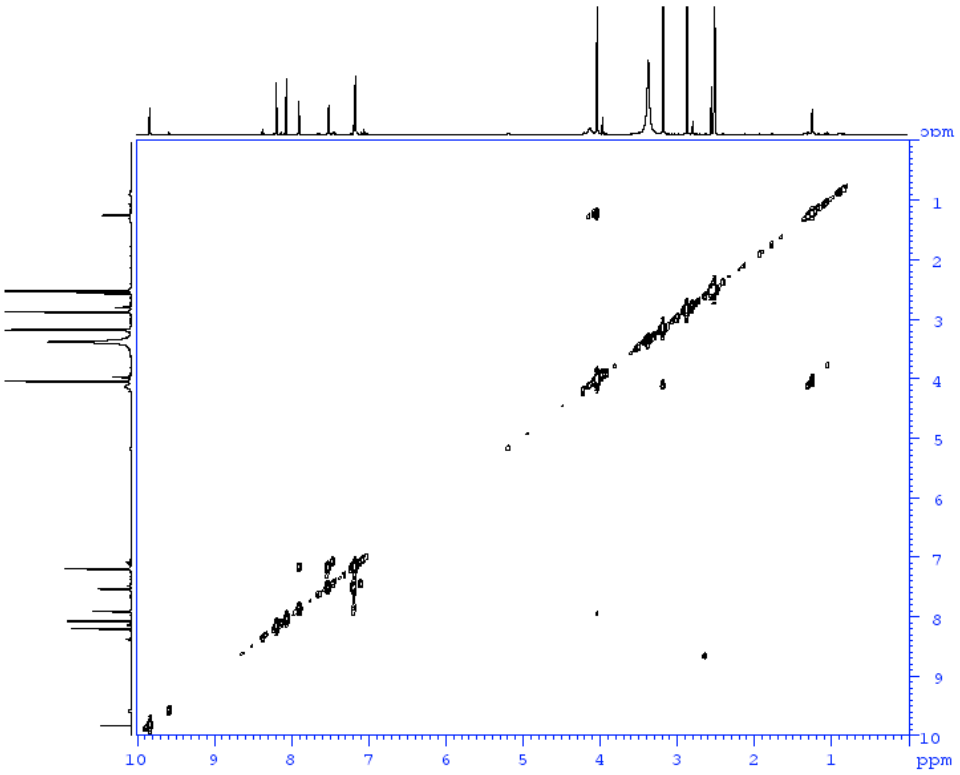

Figure S11. COSY spectrum (DMSO-d_6, 600 MHz) of lazarimide A (**7**).

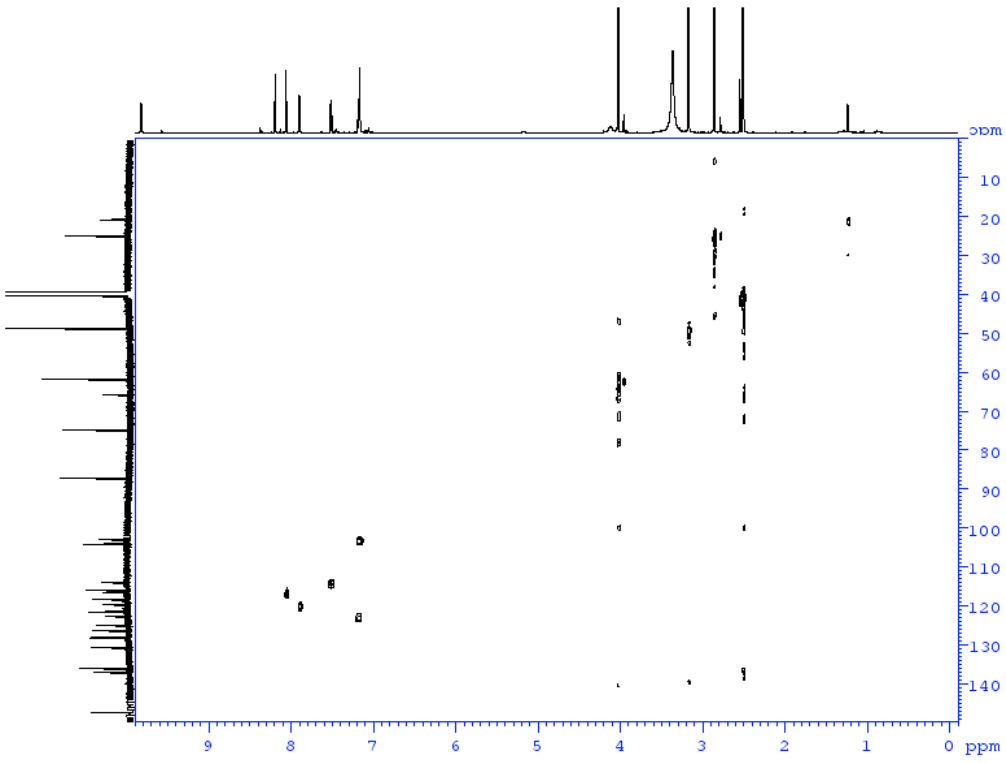

Figure S12. HMQC spectrum (DMSO-d_6, 600 MHz) of lazarimide A (**7**).

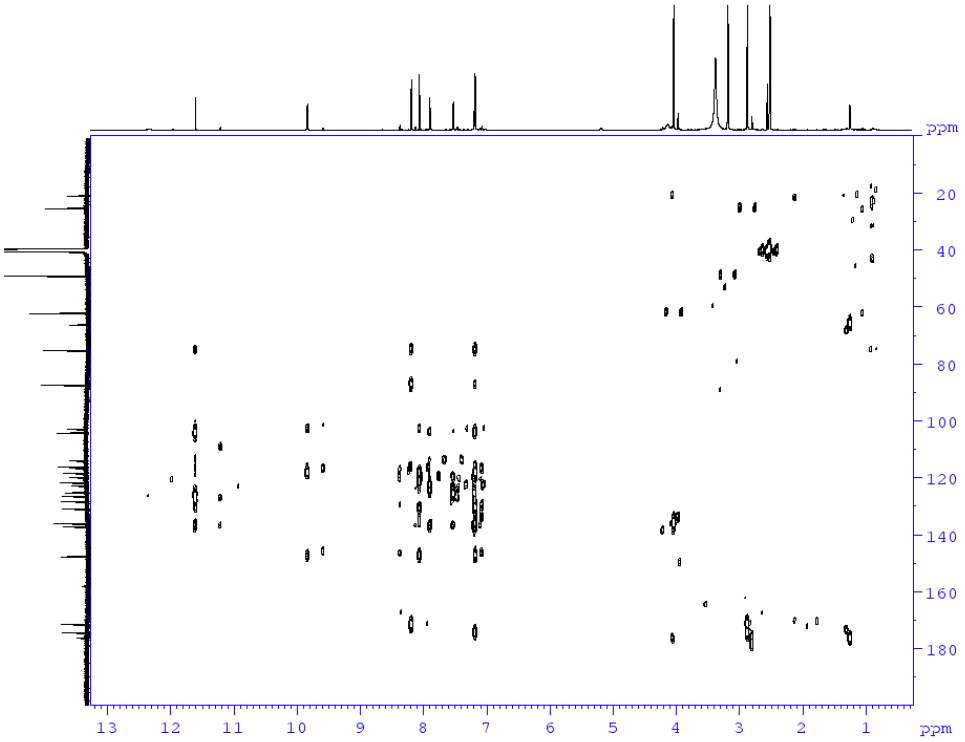

Figure S13. HMBC spectrum (DMSO-d_6, 600 MHz) of lazarimide A (**7**).

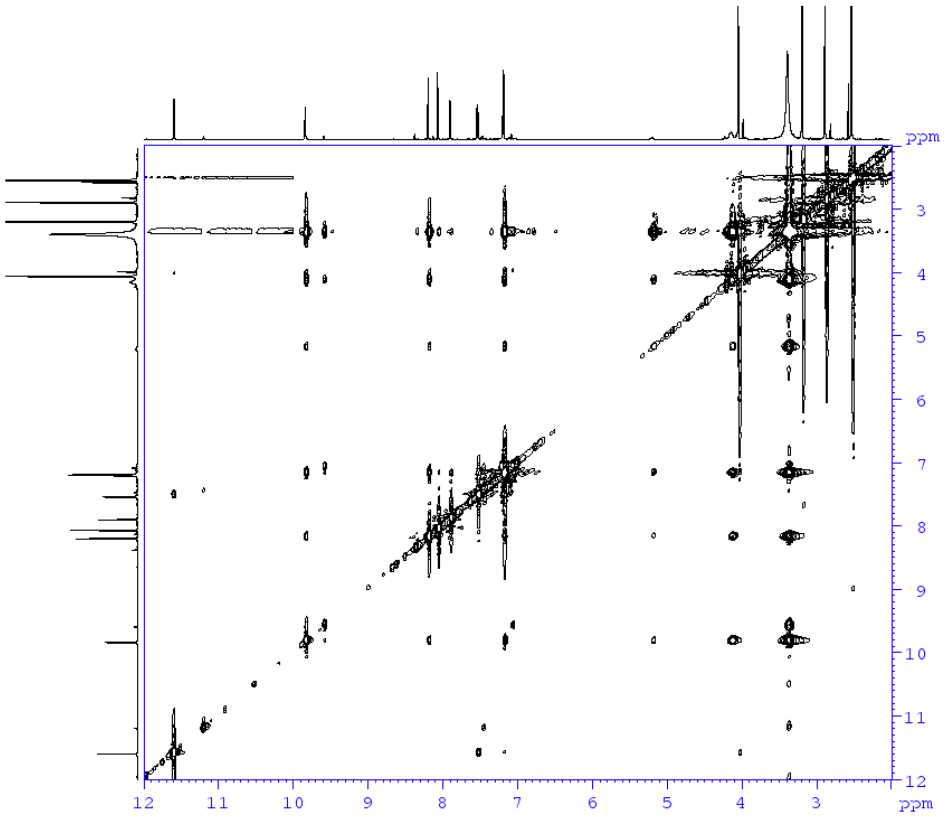

Figure S14. NOESY spectrum (DMSO-d_6, 600 MHz) of lazarimide A (**7**).

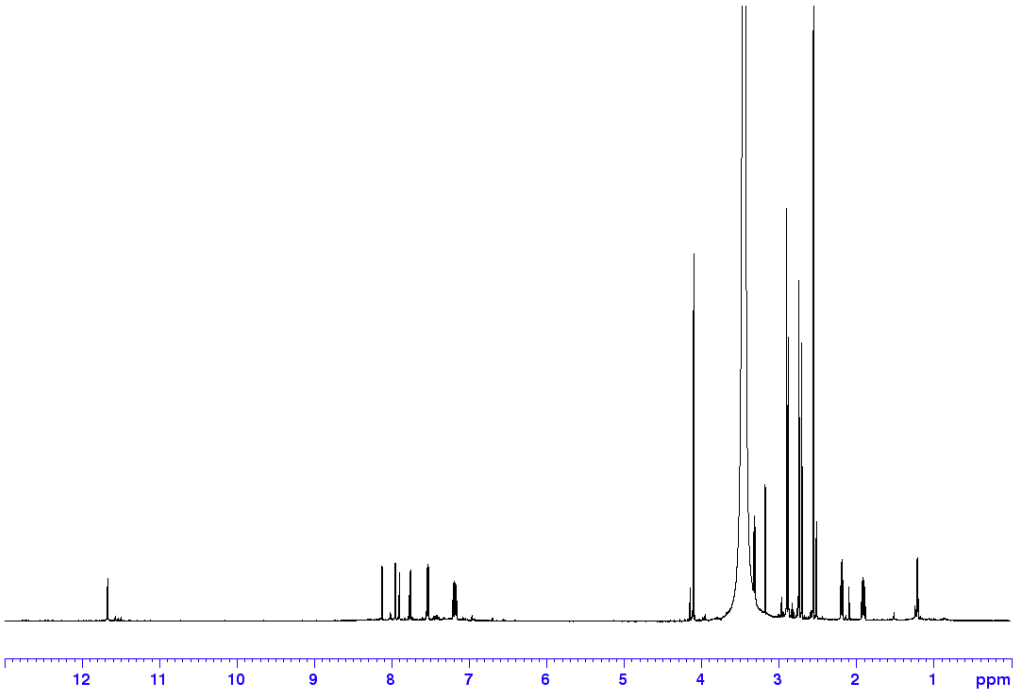

Figure S15. ^{1}H NMR spectrum (DMSO-d_6, 600 MHz) of lazarimide B (**6**).

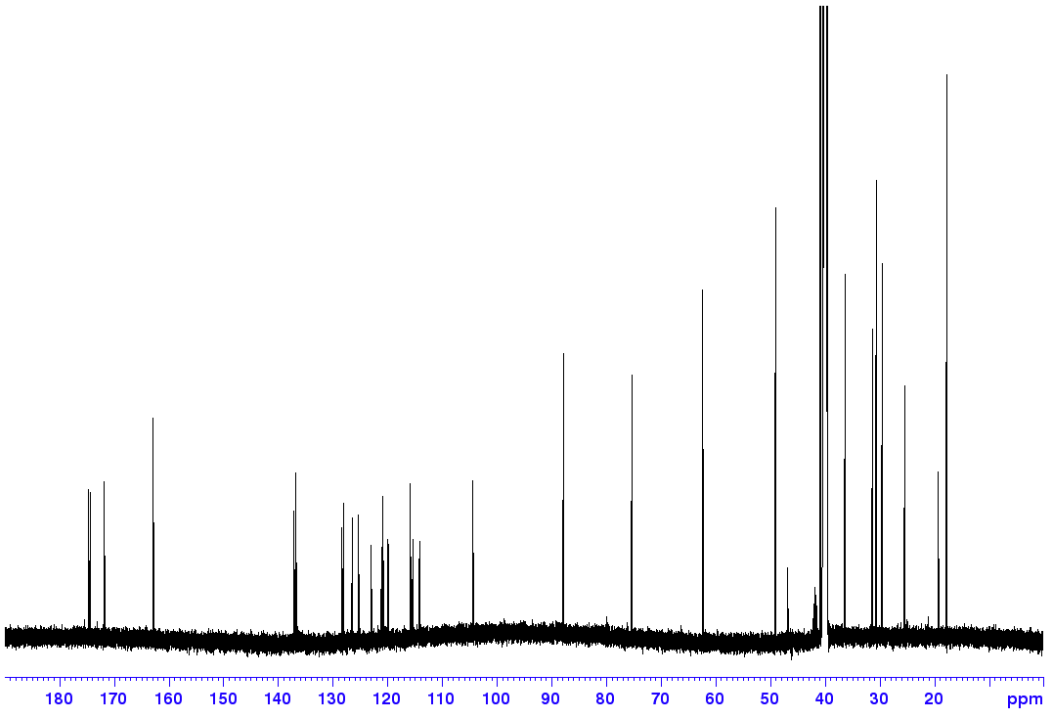

Figure S16. ^{13}C NMR spectrum (DMSO-d_6, 150 MHz) of lazarimide B (**6**).

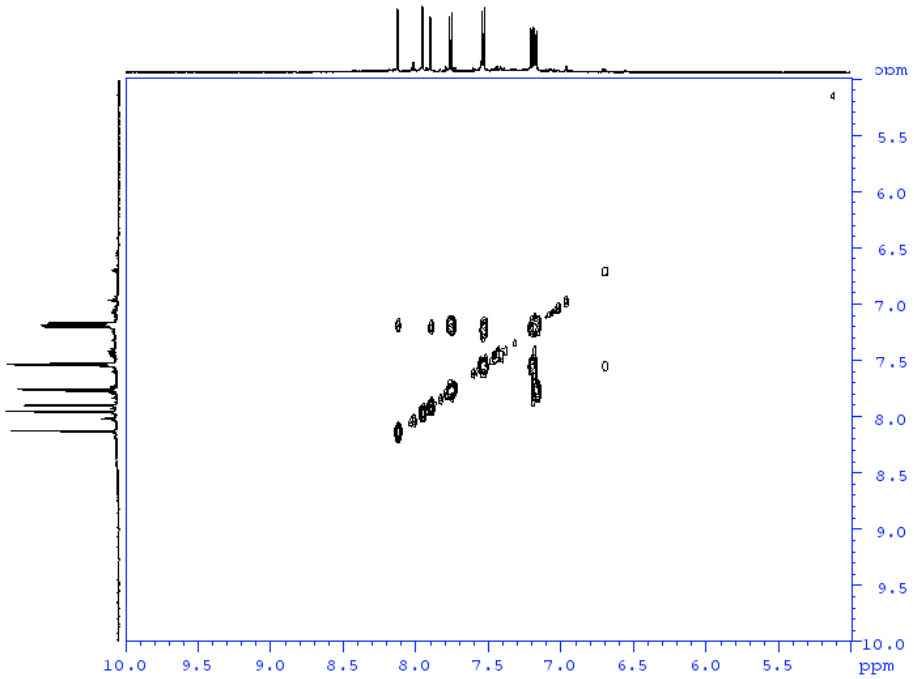

Figure S17. COSY spectrum (DMSO-d_6, 600 MHz) of lazarimide B (**6**).

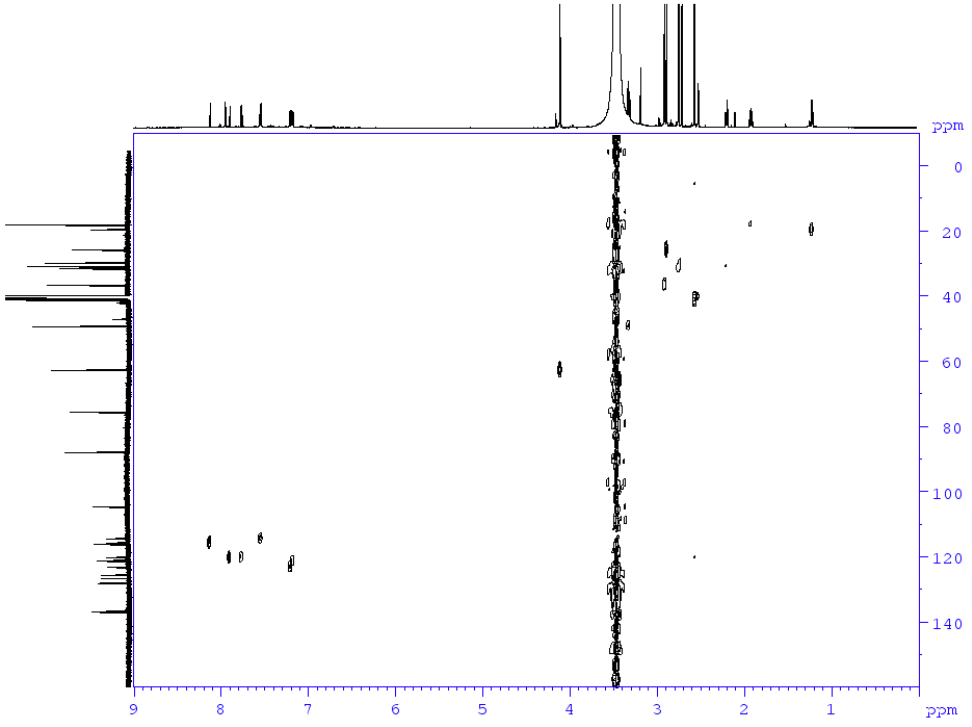

Figure S18. HMQC spectrum (DMSO-d_6, 600 MHz) of lazarimide B (**6**).

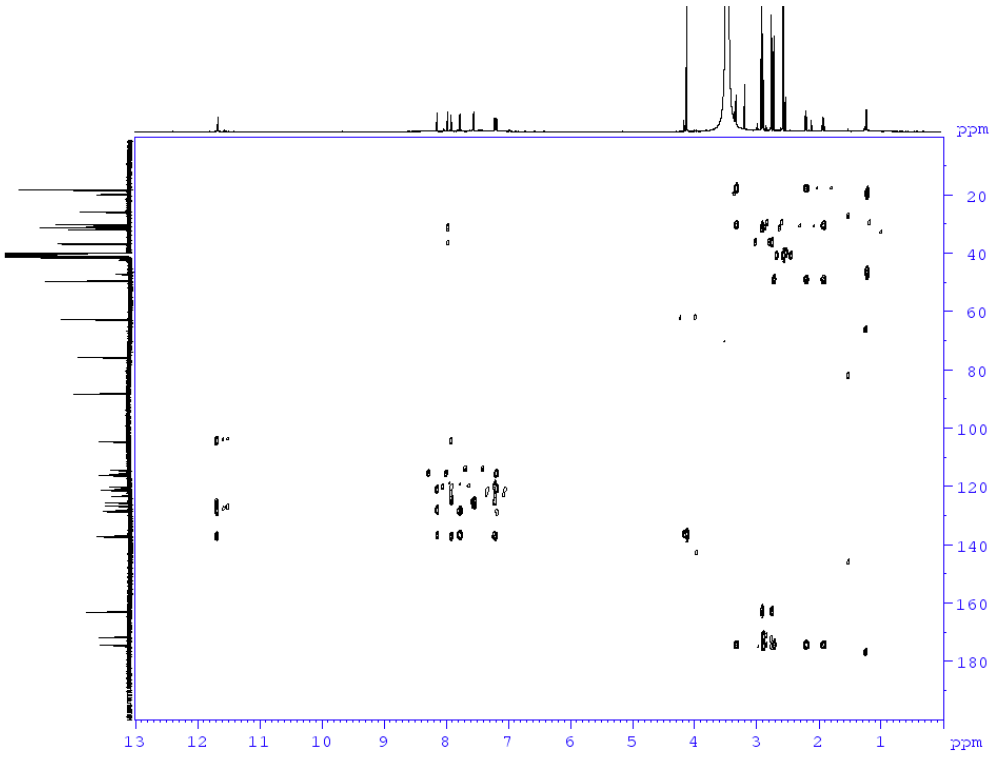

Figure S19. HMBC spectrum (DMSO-d_6, 600 MHz) of lazarimide B (**6**).

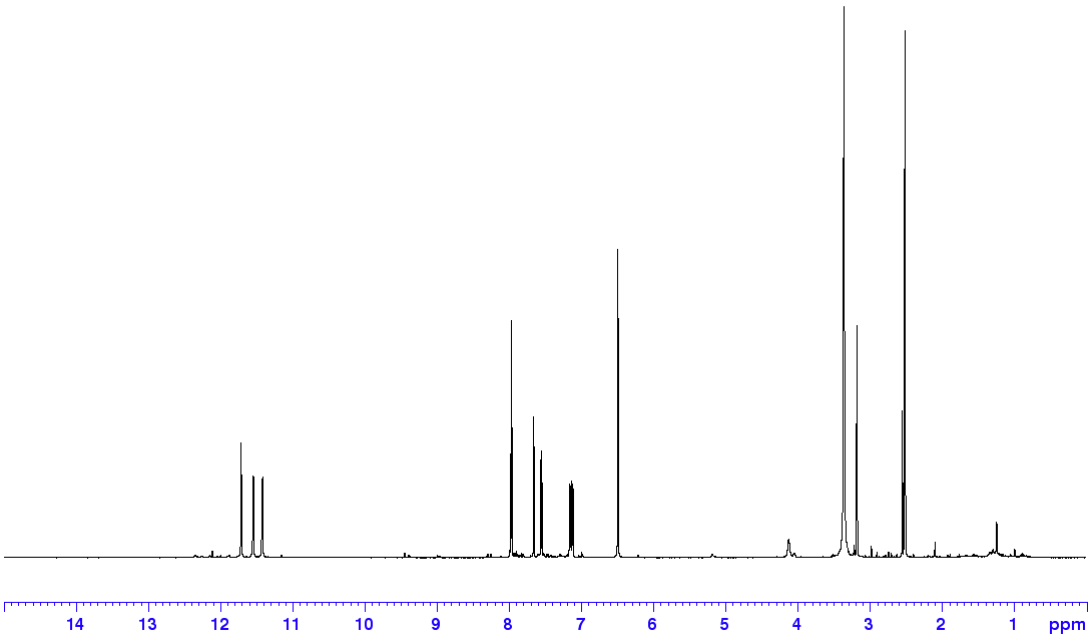

Figure S20. ^{1}H NMR spectrum (DMSO-d_6, 600 MHz) of lazarimide C (**5**).

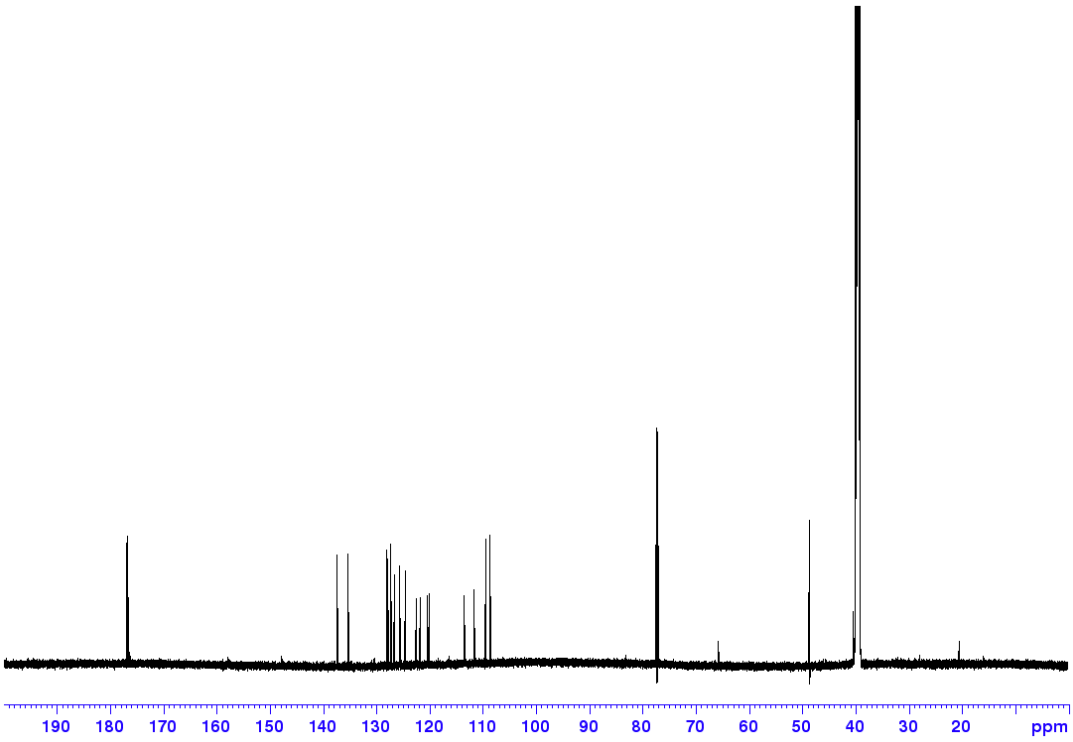

Figure S21. ^{13}C NMR spectrum (DMSO-d_6, 150 MHz) of lazarimide C (**5**).

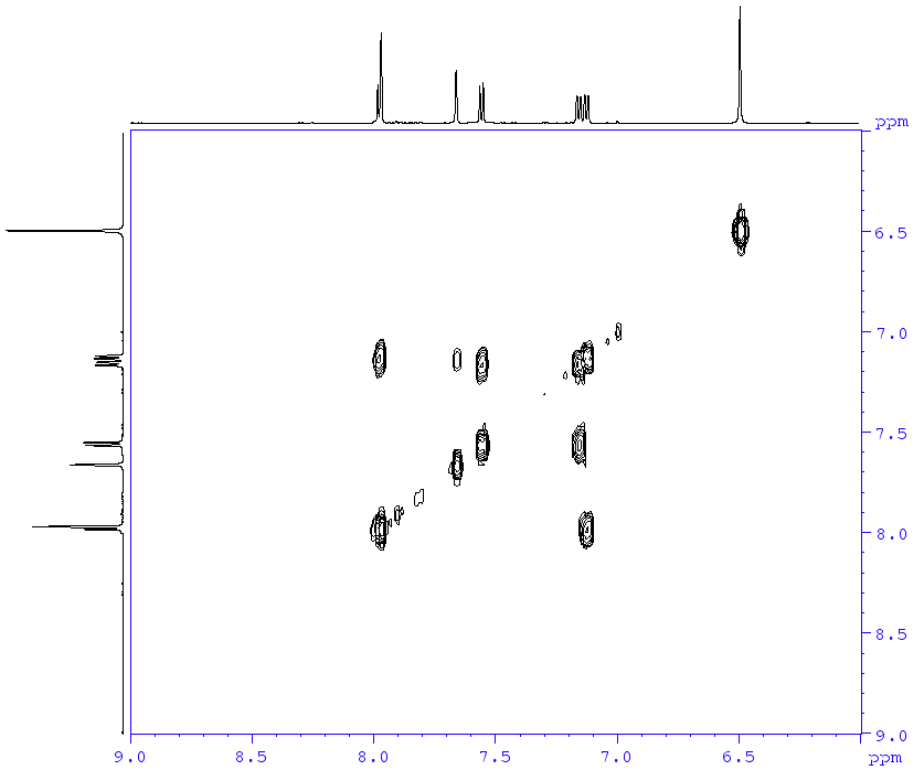

Figure S22. COSY spectrum (DMSO-d_6, 600 MHz) of lazarimide C (**5**).

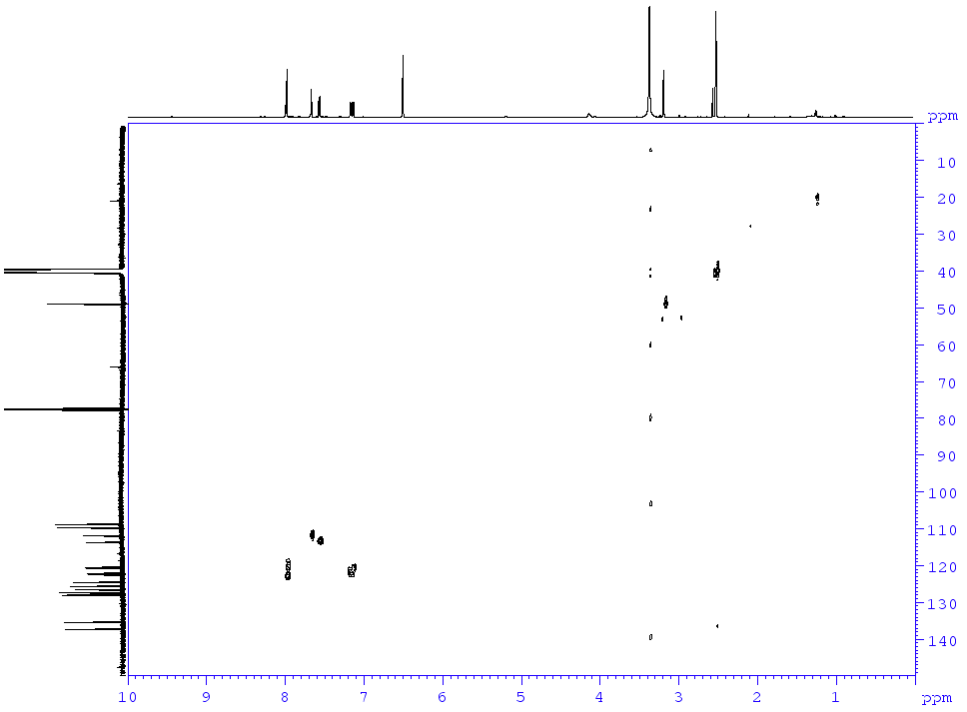

Figure S23. HMQC spectrum (DMSO-d_6, 600 MHz) of lazarimide C (**5**).

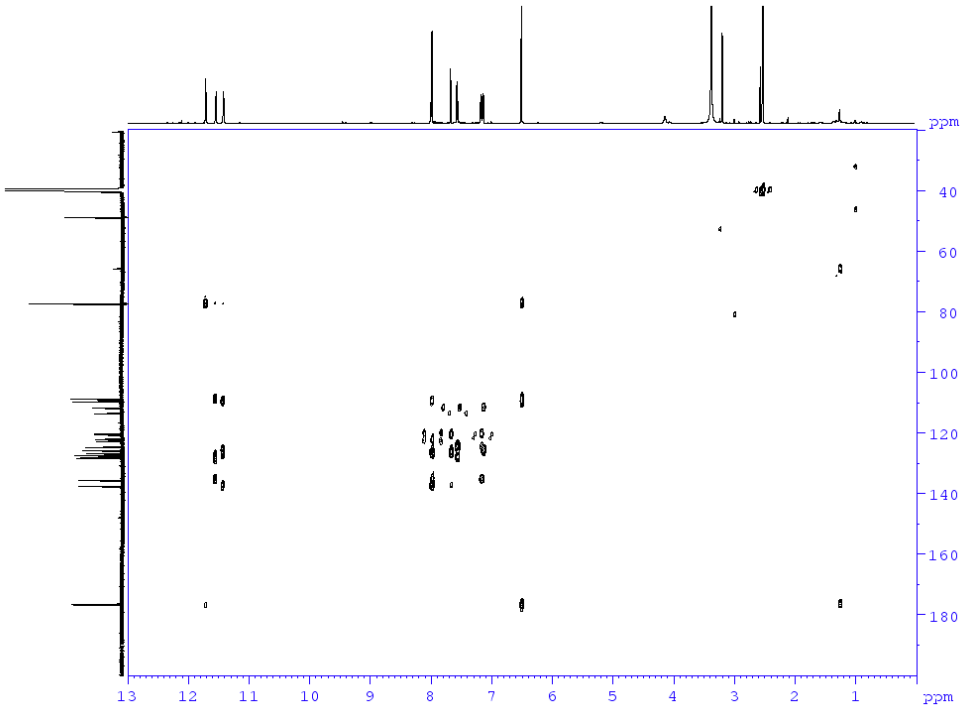

Figure S24. HMBC spectrum (DMSO-d_6, 600 MHz) of lazarimide C (**5**).

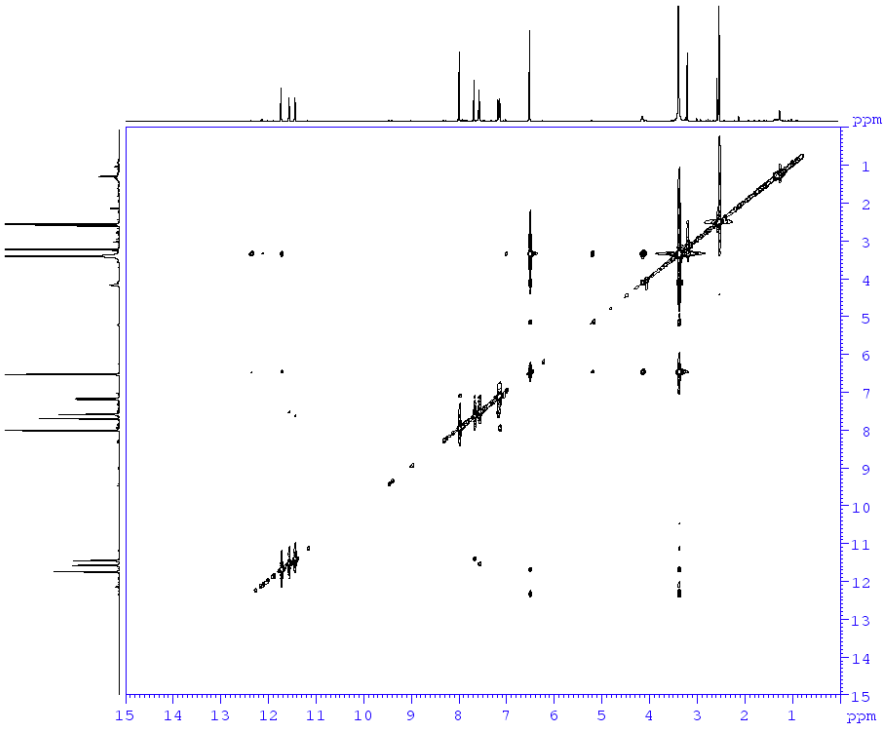

Figure S25. NOESY spectrum (DMSO-d_6, 600 MHz) of lazarimide C (**5**).

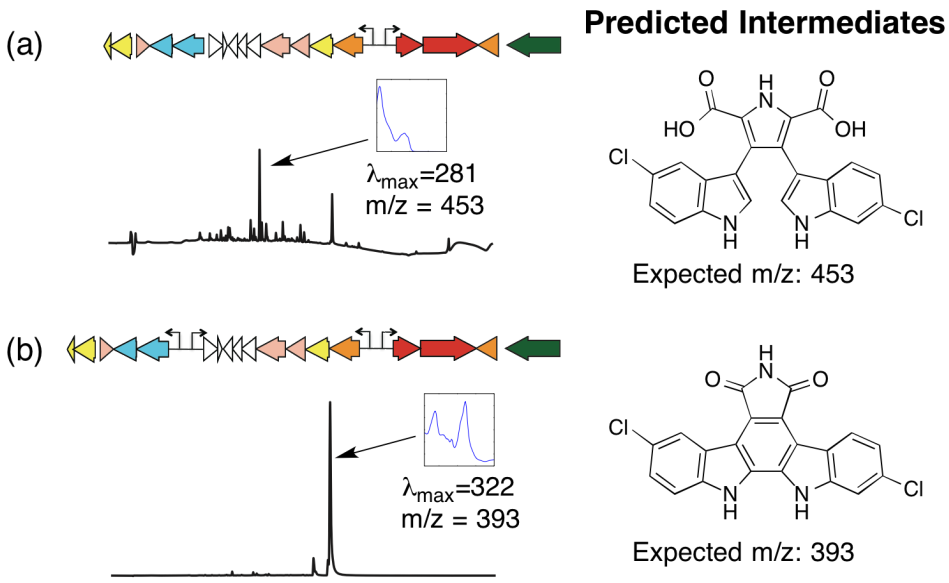

Figure S26. (a) HPLC chromatogram (measured at 210 nm) of an extract of *S. albus* harboring the Lzr gene cluster refactored with a single bi-directional promoter cassette. The arrow indicates a peak corresponding to a pathway specific metabolite not observed in extracts of *S. albus* containing the native Lzr gene cluster. The absorption spectrum and mass {*m/z* = 453 ($[M-H]^-$)} are consistent with the bioinformatically predicted di-chlorinated chromopyrrolic acid intermediate. (b) HPLC chromatogram (measured at 320 nm) of an extract of *S. albus* harboring the Lzr gene cluster refactored with two bi-directional promoter cassettes. The arrow indicates a pathway specific metabolite with an absorption spectrum and mass {(*m/z* = 453 ($[M-H]^-$)} consistent with the bioinformatically predicted di-chlorinated indolocarbazole intermediate.

Supplementary tables.

Table S1. The list of primers used for the construction of promoter cassettes

BSP1: LEU2 promoter cassette with P01 and P02

FW 5′-
GATTCCTCCTGACGTATGTATTGAACGCGGCACCCTAGCGGGCCCCCACTATCGAGTCAATTCTACTTTTTCGAC
GGTCGAGGAGAACTT-3′

RV 5′-
GTGGTGCCTCCTGGTGTTGGTGGAGACGACCCCACCCTAACCAATCCTGTCATAGCGGTCAATTGTGCTTTGTCG
ACTACGTCGTAAGGCCG-3′

BSP2: MET15 promoter cassette with P03 and P04

FW 5′-
CCGCGACTCCTTGCACATTAGGCTCCCTACAGAACCTAGGCACACACCCTCATTACGTCAATCTCGCACTCGCCA
TCCTCATGAAAACTGT-3′

RV 5′-
CCAGCTCCTCCTATCCGCTACTCCCCAGTTTCCACGCTATGGGAAGACGAGAACACAGTCAACTCTAAATAAACT
TGTGAGAGAAAGTAGGT-3′

BSP3: TRP1 promoter cassette with P05 and P06

FW 5′-
GTCCGGACCTCCTGACCAGCATTCTGGCGGTATCACTCTATAAATGAGGCCCCTCGAAGTCAACTTTCCGGAGAA
CGACATTACTATATATAT-3′

RV 5′-
GTGTTCCCCTCCCTTTGGCCTGCCTTAAGCGTTGACTCTACGCTTGAAGTCCCCTTTCGTCAATTACAACAGTGG
CAAGTGCACAAACAATAC-3′

BSP4: HIS3 promoter cassette with P07 and P08

FW 5′-
GGAAGGTCTCCTTTCACTCGGGCGGACCAGCACAACGTAGGCGACCGGTACAACAAGGTCAAATTACTGCGTAAT
TCCCGTTTTAAGAGCTT-3′

RV 5′-
GGGTCCTCCTCCTCACCTCTGGTAGGAAGTAACGACCGTACTTGCTCTCGCGCTCTCCGTCAAAATTTTATTCGA
TCCGTCGAGTTCAAGAGA-3′

BSP5: LYS2 promoter cassette with P09 and P10

FW 5′-
GCGGGACCTCCTGCGAGCAGCAAATACGTTCCGAAGGTAAGCACCATATTCAGCTGAGTCAATGTGATCCCAAGA
TTGTACTGAGAGTGCAC-3′

RV 5′-
ACGGACCTCCGGGCTAATCGCGTGATAACGAAATCGTAGGCAATCTGACTAACTGTGTCAACCAGCGAGGGCTGT
GCGGTATTTCACACCG-3′

BSP6: LEU2 promoter cassette with P11 and P12

FW 5′-
CGATCAACTCCTTGATGTTCCGATATTGCACTCACCCTAGGCCTAACGGAAAAATACGTCAACCTAGTTGCCTCG
ACGGTCGAGGAGAACTT-3′

RV 5′-
GTCTCCCCCACGATAACTACTGGGCCGACCAACCCTATCCCTATACATAGGTTTGGTCAAGCAACGCATATCGAC
TACGTCGTAAGGCCG-3′

BSP7: MET15 promoter cassette with P13 and P14

FW 5′-
GATCGTTCTCCTTCTTGGCTACTTCCGTGATCACCTACCCTAACCCCTCACCTCAGCGTTGTCAACGCGACATCG
GCCATCCTCATGAAAACTGT-3′

RV 5′-
AGCGGACCTCTATACGACATCTTTATTGCGCATATCCTAACACTCCCCAAATACATCGTCAATACGACCCACACT

TGTGAGAGAAAGTAGGT-3′

BSP8: TRP1 promoter cassette with P15 and P16

FW 5′-
TGAGGACCACCTCTCATAACGAACACGTGGCAGGTTAACCTATATTGCTTCACTCTCAACGTCAAGTGGGCAATT
AACGACATTACTATATATAT-3′

RV 5′-
AGCGGACCTCTATGGCTTGACGGACCACCAGCGACGCTACCACCCGATGTCAGGGGCGTCAAACTGATCACCGGC
AAGTGCACAAACAATAC-3′

BSP9: HIS3 promoter cassette with P17 and P18

FW 5′-
ATCGAATTCCTCGGGAGGACCCGTATTCGGTCCTCATGCTACAGACCGGGACCCCGTACGTCAAAGTCCACCGAA
ATTCCCGTTTTAAGAGCTT-3′

RV 5′-
CGACGTACTGCCTCCGTTGTGTAGACCAGACCTGACGACTCTATAATGGAATATTATTTTAGTCAAACCCTACGC
CGATCCGTCGAGTTCAAGAGA-3′

BSP10: LYS2 promoter cassette with P19 and P20

FW 5′-
TGCCGCACTCCTCACGCCCAGCAACTTCGTCACACCGTATGATCAGAAAGCCGGCTTGTCAACTGCGATGTAAGA
TTGTACTGAGAGTGCAC-3′

RV 5′-
GGCACCTCGATGCTCGCCGGCGCCCGACCGCACCGTACCCGGAATAGTGGCGGCGGTCAACTGCAGCGGACTGTG
CGGTATTTCACACCG-3′

BSP11: KanMX promoter cassette with P21 and P22

FW 5′-
GAACTCGCTACCTCTCGGGCTGGCCAGAGCAGGCCAGACTCTATCTCTACACCCCCGCGGCGTCAAGGACACAGA
CCGTACGCTGCAGGTCGAC-3′

RV 5′-
GTCAACGCATCTCCCGGGTCGGTCCCGAAGATCGACACTCTAGTTATACCCCTCGATCCTGTCAAACGAACCTGC
ATCGATGAATTCGAGCTCG-3′

BSP12: KanMX promoter cassette with P23 & ErmE

FW 5′-
GAACTCGCTACCTCTCGGGCTGGCCAGAGCAGCTTTGATGGTAGCAACTCAGACCCACGGGGTCAAACACATGTG
ACGTACGCTGCAGGTCGAC-3′

RV 5′-
GTCAACGCATCTCCCGGGTCGGTCCCGAAGAGTCAGATCCTCCCCGCACCTCTCGCCAGCCGTCAAGATCGACCG
CATCGATGAATTCGAGCTCG-3′

Table S2. The list of primers used for PCR-based deletion of the DNL4 gene

Primers used for construction of the Dnl4 gene deletion cassette

FW primer:
5′-AATAAATACTAAAATAAAAATCTAGAACTGAAGGAAATAGTAACGGATTATTTAGGTATGCGTACGCTGCAGGTCGAC-3′
RV primer:
5′-ATATGTAGGATAGTATTAAATAAACTTCAAAAAATTAAGCCTCCGCAAAACGCACCATCAATCGATGAATTCGAGCTCG-3′

Primers used for confirmation of the DNL4 deletion

Dnl4KO_700_1_FW : 5′-CTGACACATCAGAGAGTG-3′
Dnl4KO_700_1_RV : 5′-GTCAAGACTGTCAAGGAG-3′
Dnl4KO_700_2_FW : 5′-GCTATACTGCTGTCGATTC-3′
Dnl4KO_700_2_RV : 5′-GTTGCTTCTCAGGACATAG-3′

Table S3. The list of primers used for the promoter exchange of the Reb gene cluster

Homology sequences used to replace the first bidirectional promoters in the Reb gene cluster

FW primers: 5′-CCTCGCCCGGAGTCGTCGCCACAAGAACTCGTACCACCAT+20 bp primer sequences-3′
RV primers: 5′-CGGCGCCGAGAATGGTGATCTTCTTGCGCCTGTGTGACAT+20 bp primer sequences-3′

Screening primers from promoter cassettes

P01: 5′-GTGCCGCGTTCAATACATAC-3′
P02: 5′-GACAGGATTGGTTAGGGTGG-3′
P03: 5′-GCCTAATGTGCAAGGAGTCG-3′
P04: 5′-GGGAGTAGCGGATAGGAGG-3′
P04: 5′-GGGAGTAGCGGATAGGAGG-3′
P05: 5′-GAATGCTGGTCAGGAGGTCC-3′
P06: 5′-AGTCAACGCTTAAGGCAGGC-3′
P07: 5′-CGCCTACGTTGTGCTGGTCC-3′
P08: 5′-CGCGAGAGCAAGTACGGTCG-3′
P09: 5′-GGAACGTATTTGCTGCTCGC-3′
P10: 5′-GTTATCACGCGATTAGCCCG-3′
P11: 5′-GTTAGGCCTAGGGTGAGTGC-3′
P12: 5′-ATGCGTTGCTTGACCAAACC-3′
P13: 5′-AGGTGATCACGGAAGTAGCC-3′
P14: 5′-GATGTCGTATAGAGGTCCGC-3′
P15: 5′-CGTTATGAGAGGTGGTCCTC-3′
P16: 5′-CCGTCAAGCCATAGAGGTCC-3′
P17: 5′-CGAATACGGGTCCTCCCGAG-3′
P18: 5′-TACACAACGGAGGCAGTACG-3′
P19: 5′-GTTGCTGGGCGTGAGGAGTG-3′
P20: 5′-CGCCGGCGAGCATCGAGGTG-3′
P21&P23: 5′-GGCCAGCCCGAGAGGTAGCG-3′
P22&ermE: 5′-CTTCGGGACCGACCCGGGAG-3′

Screening primers from the Reb gene cluster

Reb_1: 5′-ACCACGGCGGCGGCGTGAAG-3′
Reb_2: 5′-CCAGCGCGTCGACGAGCTGG-3′

Primers used for amplification of the unidirectional MET15 promoter cassette

FW primers: 5′-CGAGGCCGGCTACCTGTTGCTCGGCGCACGGCGGCCCTGAGCCATCCTCATGAAAACTGT-3′
RV primers: 5′-GGATATCCGGCACTAACGCGGCATTTCCGAAGCGCTTCATCCAGCTCCTCCTATCCGCTA-3′

Primers used for amplification of the bidirectional MET15 promoter cassette

FW primers: 5′-CGAGGCCGGCTACCTGTTGCTCGGCGCACGGCGGCCCTGACCGCGACTCCTTGCACATTA-3′
RV primers: 5′-GGATATCCGGCACTAACGCGGCATTTCCGAAGCGCTTCATCCAGCTCCTCCTATCCGCTA-3′

Primer sets used for screening of insertion of the MET15 unidirectional and bidirectional promoter cassettes

Reb_3 : 5′-GGTCGACGACGCCACGGACC-3′
Reb_4 : 5′-CGGCGACCAGCTCCTCGGCC-3′
P03 : 5′-GCCTAATGTGCAAGGAGTCG-3′
P04 : 5′-GGGAGTAGCGGATAGGAGG-3′
MET_1 : 5′-TCGGTTATTATGTTACACAG-3′

Table S4. The list of primers used for simultaneous exchanges of multiple promoter cassettes

Primers used for PCR amplification of promoter cassettes with 500 bp homology arms

RebLEU2	FW: 5′-GCCGACCGGAGGTCCCGCAT-3′	RV: 5′-ACCACGGCGAGCAGGTCGGC-3′
RebMET15	FW: 5′-GGCTCGCCCACCGGGTGAGC-3′	RV: 5′-GTCCACTGCAGGTCGTCCAG-3′
RebTRP1	FW: 5′-CACGACCAGCCCGGGCCCGA-3′	RV: 5′-GTCGGTCACGAACGTGGCCT-3′

Primers used for PCR-based genotyping of multiple promoter exchange constructs

a	Reb_1:	5′-ACCACGGCGGCGGCGTGAAG-3′	P01 :	5′-GTGCCGCGTTCAATACATAC-3′
b	P02 :	5′-GACAGGATTGGTTAGGGTGG-3′	Reb_2:	5′-CCAGCGCGTCGACGAGCTGG-3′
c	Reb_3:	5′-GGTCGACGACGCCACGGACC-3′	MET_1:	5′-TCGGTTATTATGTTACACAG-3′
d	P04 :	5′-GGGAGTAGCGGATAGGAGG-3′	Reb_4:	5′-CGGCGACCAGCTCCTCGGCC-3′
e	Reb_5:	5′-CCCCCAGCGCCACCAGGATC-3′	P15 :	5′-CGTTATGAGAGGTGGTCCTC-3′
f	TRP_1:	5′-GGAGGTGTGGAGACAAATGG-3′	Reb_6:	5′-ACGCCGGCGCCGGGGGAGAC-3′

Table S5. The list of primers used for the promoter exchange of the Tam gene cluster

Primers for the LEU2 promoter cassette

FW: 5′-ACACCCTCAGCAGGGCCACCGCCCAACGCTCCCATTTCATGATTCCTCCTGACGTATGTA-3′
RV: 5′-ACTTGATCCCGTCCACCCCGATGAAAGGTCTGCTGCCCATGTGGTGCCTCCTGGTGTTGG-3′

Primers for the MET15 promoter cassette

FW: 5′-TGACGCGCACACCGGTGCGCCCCACTATGCGGTACTGCATCCGCGACTCCTTGCACATTA-3′
RV: 5′-CTGCCCGCTTGGGTTTGGGCCCGTCGCTGTCCTTCACCACCCAGCTCCTCCTATCCGCTA-3′

Primers for the TRP1 promoter cassette

FW: 5′-CACCGACGACGAGTACCCGCGTACTCTCCACACCGGACATTGAGGACCACCTCTCATAAC-3′
RV: 5′-CTTCGTCGGATGGTCGTTGACACTCTTTGTCGTTTGTCACAGCGGACCTCTATGGCTTGA-3′

Primers for the HIS3 promoter cassette

FW: 5′-CACCGGACAGCAGCGCGGACAGCCTCGGCCGGTCCAGCACGGAAGGTCTCCTTTCACTCG-3′
RV: 5′-CCAGCCACGCCGCGGTGCCGCTGACCCTGCTCGCCGAGACGATCCGTCGAGTTCAAGAGA-3′

Primers used to generate promoter cassettes with 500 bp homology arms

LEU2	FW: 5′-GATGCGCACGACGATCGGCA-3′	RV: 5′-GCCATCGCCGCCATCAGCGA-3′
MET15	FW: 5′-TGGGCCTGCACGATCCGGTA-3′	RV: 5′-ATGCAGAGGTTGCCCACGCC-3′
TRP1	FW: 5′-CCGATGGCACCCGCGGGCCC-3′	RV: 5′-AGCGGCTCGCCGCGCCACAG-3′

Primers used for PCR-based genotyping of promoter exchange constructs

LEU2	Tam_1:	5′-CTGTCCGCCCCTGGTCACTC-3′	P01 :	5′-GTGCCGCGTTCAATACATAC-3′
	P02 :	5′-GACAGGATTGGTTAGGGTGG-3′	Tam_2:	5′-GGGTGGTGAACGCCCGCACC-3′
MET15	Tam_3:	5′-CGGCGCGGCTCGTGGTGATC-3′	P03 :	5′-GCCTAATGTGCAAGGAGTCG-3′
	P04 :	5′-GGGAGTAGCGGATAGGAGG-3′	Tam_4:	5′-TACCAGCCGACGCGGAGTAC-3′
TRP1	Tam_5:	5′-CCGATGGCACCCGCGGGCCC-3′	P15 :	5′-CGTTATGAGAGGTGGTCCTC-3′
	P16 :	5′-CCGTCAAGCCATAGAGGTCC-3′	Tam_6:	5′-AGCGGCTCGCCGCGCCACAG-3′
HIS3	Tam_7:	5′-CCCGGTCGACGATCTCCGTC-3′	P07 :	5′-CGCCTACGTTGTGCTGGTCC-3′
	HIS_2:	5′-GTCATTCTGAACGAGGCGCG-3′	Tam_8:	5′-CCGGTGAGGCGCACCAGGTG-3′

Table S6. The list of primers used for the promoter exchange of the Lzr gene cluster

Primers for generation of the pathway specific Lzr TAR capture vector

P153-prox-F	AAAAGCTAGCCGTGATGGAGATCGTCGAC
P153-prox-R	CTTATGCCGCAACGTCTGTCGTTAACCTGCTTGTAGATTCCATCGGC
P292-dist-F	GCCGATGGAATCTACAAGCAGGTTAACGACAGACGTTGCGGCATAAG
P292-dist-R	AAAAGCATGCCGTCGTCATGTCGTTCGTG

Primers for the LEU2 promoter cassette

Lzr Promoter Site 1
FW primers: 5′-CGCCGAGGACGACGACCTTCCTGATCCGATGATCTTCCAC+20bp primer sequences-3′
RV primers: 5′-TCCCCGCACCGAGAACCGTGACCTTCTTGCGCGCTGACAT+20bp primer sequences-3′

Lzr Promoter Site 2
FW primers: 5′-CGCCGACGACGAGCACGTCGGTCGTGAGCTGGGAGGTCAT+20bp primer sequences-3′
RV primers: 5′-CGGTGGTGCGCTGCTGGGTTTCGGCGGTGCTCGTGGGCAT+20bp primer sequences-3′

Lzr Promoter Site 3
FW primers: 5′-CCCCCACCACGAGTACGTCGCAGTCGTGTTCGTCGCGCAT+20bp primer sequences-3′
RV primers: 5′-GCTCGGCCAGATCGTCGAAATAGGCTTCCGGTGCGCTCAT+20bp primer sequences-3′

Lzr Promoter Site 4
FW primers: 5′-GCCAGACCTTTTTGCCGTCGGGGAGCTGGATCTGTTCCAC+20bp primer sequences-3′
RV primers: 5′-GAGCGGCACAACCACTCACGACCCCACCTGCGCGAACGTG+20bp primer sequences-3′

Primers used for PCR-based genotyping of promoter exchange constructs

lzrP1	FW: 5′-TGGTCGTAGGTCTCGCCGT-3′	RV: 5′-TGTCGGTGAGCGGCATCG-3′
lzrP2	FW: 5′-GTCACAGGCGATCAGGTA-3′	RV: 5′-AGCCAGAACACCTCGTTGA-3′
lzrP3	FW: 5′-GAGGTGCGCGTCGAAGT-3′	RV: 5′-GAAGAACGCGTGCAGGTC-3′
lzrP4	FW: 5′-GTGAACACCATCGAGGCG-3′	RV: 5′-TTCTGGTCATCTCGGCGTTGC-3′

Table S7: NMR spectroscopic data for lazarimide A (**7**) in DMSO-d_6

No.	Lazarimide A (**7**)				
	δ_C [b]	δ_H [a]	*J* in Hz	HMBC	NOE
1	113.6	7.51	d (8.6)	3, 4a	NH,
2	122.3	7.17	dd (8.6, 1.7)	3, 4, 13a	
3	124.7				
4	119.4	7.88	d (1.7)	2, 4b, 13a	
4a	126.0				
4b	103.8				
4c	74.8				
5	174.2				
6					
7	171.4				
7a	87.1				
7b					
7c	130.4				
8	116.1	8.04	s	7c, 9, 10, 11a	
9	118.0				
10	147.2				
11	102.5	7.16	s	7c, 9, 10, 12	10-OH
11a	121.2				
12	135.7				
12a	115.7				
12b	127.9				
13		11.59	s		1
13a	136.6				
14	24.8	2.86	s	5, 7	
12-OMe	61.67	4.02	s	12	11, 13(NH)
C4c-OH		7.16	s	4c, 4b, 5, 7a	7a-OH
C7a-OH		8.17	s	4c, 7a, 7	11, 4c-OH,
C10-OH		9.81	s	9, 10, 11	11, 7a-OH

[a] recorded at 600 MHz, [b] recorded at 150 MHz, [a,b] signals were referenced to the DMSO-d_6 solvent signals (δ_H 2.50 and δ_H 39.51).

Table S8: NMR spectroscopic data for lazarimides B (**6**) and C (**5**) in DMSO-d_6

No.	lazarimide B (**6**)			lazarimide C (**5**)		
	δ_C[b]	δ_H[a]	*J* in Hz	δ_C[b]	δ_H[a]	*J* in Hz
1	113.8	7.52	d (8.6)	113.5	7.54	d (8.6)
2	122.7	7.16	dd (1.9, 8.6)	121.8	7.14	dd (1.5, 8.6)
3	124.9			124.6		
4	119.5	7.89	d (1.9)	120.1	7.95	d(1.5)
4a	126.0			128.1		
4b	103.9			108.7		
4c	74.9			77.1		
5	174.3			176.7		
6					11.7	s
7	171.4			176.9		
7a	87.4			77.3		
7b				109.5		
7c	136.5			126.6		
8	115.0	8.11	d (1.8)	122.5	7.96	d (7.2)
9	128.0			120.4	7.11	dd (1.9, 7.2)
10	120.7	7.19	dd (8.6, 1.8)	125.7		
11	119.5	7.75	d (8.6)	111.6	7.64	d (1.9)
11a	120.5			137.4		
12	136.3				11.42	s
12a	115.3			127.3[c]		
12b	127.7			127.9[c]		
13		11.66	s		11.54	s
13a	136.8			135.4		
14	25.0	2.86	s			
12-OMe	62.0	4.09	s			
C4c-OH					6.48	s
C7a-OH					6.48	s
C10-OH						

[a] recorded at 600 MHz, [b] recorded at 150 MHz, [a,b] signals were referenced to the DMSO-d_6 solvent signals (δ_H 2.50 and δ_H 39.51), [c] these signals could be interchanged.

Table S9. Crystal data and structure refinement for compound **5**.

Empirical formula	$C_{22}H_{19}Cl_2N_3O_6$	
Formula weight	492.30	
Temperature	193(2) K	
Wavelength	0.71073 Å	
Crystal system	Monoclinic	
Space group P2(1)		
Unit cell dimensions	a = 6.9892(8) Å	a= 90°.
	b = 27.565(3) Å	b= 95.376(3)°.
	c = 10.8400(13) Å	g = 90°.
Volume	2079.2(4) Å3	
Z 4		
Density (calculated)	1.573 Mg/m^3	
Absorption coefficient	0.361 mm^{-1}	
F(000) 1016		
Crystal size	0.15 x 0.10 x 0.05 mm^3	
Theta range for data collection	2.40 to 21.97°.	
Index ranges	-7≤h≤7, -26≤k≤29, -11≤l≤11	
Reflections collected	9668	
Independent reflections	5008 [R(int) = 0.0506]	
Completeness to theta =	21.97° 99.8 %	
Absorption correction	Semi-empirical from equivalents	
Max. and min. transmission	0.9822 and 0.9479	
Refinement method	Full-matrix least-squares on F2	
Data / restraints / parameters	5008 / 1 / 595	
Goodness-of-fit on F2	1.029	
Final R indices [I>2sigma(I)]	R1 = 0.0649, wR2 = 0.1386	
R indices (all data)	R1 = 0.1170, wR2 = 0.1608	
Absolute structure parameter	-0.02(12)	
Largest diff. peak and hole	0.338 and -0.345 e.$Å^{-3}$	

Table S10. Atomic coordinates (x 10^4) and equivalent isotropic displacement parameters ($Å^2$x 10^3). U(eq) is defined as one third of the trace of the orthogonalized Uij tensor.

	x	y	z	U(eq)
Cl(1)	5531(4)	5052(1)	6130(3)	52(1)
Cl(2)	10458(4)	9739(1)	9690(2)	51(1)
O(1)	11208(9)	7516(3)	10425(7)	46(2)
O(2)	8940(11)	8168(3)	11820(6)	47(2)
O(3)	4742(11)	6964(3)	10561(6)	45(2)
O(4)	9054(9)	6755(2)	10945(5)	34(2)
N(1)	6467(12)	7634(3)	11238(7)	35(2)
N(2)	7374(11)	6870(3)	6694(8)	34(2)
N(3)	8258(9)	7988(3)	6920(7)	22(2)
C(1)	9151(14)	7577(3)	10135(9)	29(3)
C(2)	8270(16)	7839(4)	11134(10)	37(3)
C(3)	6210(18)	7202(4)	10607(9)	36(3)
C(4)	8107(15)	7078(3)	10064(9)	28(3)
C(5)	7781(14)	6866(4)	8778(9)	28(3)
C(6)	7218(16)	6390(4)	8403(10)	39(3)
C(7)	6905(14)	5941(4)	8974(11)	39(3)
C(8)	6388(16)	5540(4)	8281(11)	43(3)
C(9)	6162(14)	5575(4)	6959(11)	35(3)
C(10)	6455(15)	6002(4)	6358(10)	39(3)
C(11)	6978(14)	6403(4)	7074(10)	31(3)
C(12)	7837(13)	7145(3)	7758(8)	21(2)
C(13)	8282(14)	7645(4)	7853(9)	31(3)
C(14)	8753(13)	8430(4)	7424(9)	30(3)
C(15)	8852(16)	8870(4)	6856(9)	39(3)
C(16)	9380(15)	9274(4)	7551(10)	43(3)
C(17)	9822(14)	9216(4)	8841(10)	35(3)
C(18)	9701(14)	8790(4)	9431(10)	32(3)
C(19)	9146(13)	8371(4)	8716(9)	27(3)
C(20)	8855(13)	7864(4)	8988(9)	27(3)
Cl(3)	684(4)	4216(1)	7251(2)	43(1)
Cl(4)	4024(4)	9095(1)	5577(3)	51(1)
O(5)	1029(10)	7351(2)	3499(5)	37(2)
O(6)	5297(12)	7123(3)	3860(7)	46(2)
O(7)	1047(12)	5942(3)	2539(6)	52(2)
O(8)	-1187(11)	6582(2)	3973(6)	47(2)
N(4)	3520(15)	6453(3)	3177(7)	45(3)
N(5)	1833(12)	6071(3)	7452(7)	31(2)
N(6)	2769(11)	7192(3)	7720(7)	27(2)
C(21)	2008(15)	7017(3)	4372(9)	32(3)
C(22)	3822(17)	6884(4)	3795(9)	37(3)
C(23)	1709(18)	6260(4)	3205(11)	41(3)
C(24)	835(15)	6536(4)	4281(9)	35(3)
C(25)	1164(14)	6224(3)	5440(9)	25(2)
C(26)	911(13)	5726(4)	5633(9)	29(3)
C(27)	339(16)	5319(4)	4876(9)	39(3)
C(28)	241(15)	4859(4)	5414(10)	43(3)
C(29)	721(15)	4809(3)	6698(9)	29(3)
C(30)	1217(15)	5183(4)	7459(9)	36(3)
C(31)	1293(14)	5641(4)	6920(9)	28(3)
C(32)	1806(13)	6426(4)	6556(8)	25(2)
C(33)	2262(13)	6930(4)	6682(9)	27(3)

C(34)	3140(14)	7670(4)	7380(10)	30(3)
C(35)	3643(12)	8070(4)	8119(9)	31(3)
C(36)	3912(13)	8501(4)	7572(10)	30(3)
C(37)	3693(15)	8528(4)	6257(11)	38(3)
C(38)	3164(13)	8149(4)	5514(9)	32(3)
C(39)	2869(13)	7693(4)	6065(9)	28(3)
C(40)	2310(14)	7219(3)	5662(9)	27(3)
O(1W)	2122(10)	6232(3)	10131(6)	45(2)
O(2S)	3733(12)	8224(3)	12243(8)	66(2)
C(4S)	4253(19)	8737(4)	12227(12)	59(4)
O(2W)	7924(11)	7878(3)	4238(6)	49(2)
O(1S)	6260(12)	5880(3)	2178(8)	72(3)
C(2S)	4730(20)	5130(5)	1701(13)	77(4)
C(3S)	4694(17)	8925(5)	10965(11)	72(4)
C(1S)	6220(20)	5377(5)	2464(14)	84(5)

Table S11. Bond lengths [Å] and angles [°].

Cl(1)-C(9)	1.736(10)
Cl(2)-C(17)	1.745(10)
O(1)-C(1)	1.452(11)
O(2)-C(2)	1.237(12)
O(3)-C(3)	1.215(12)
O(4)-C(4)	1.422(11)
N(1)-C(3)	1.376(12)
N(1)-C(2)	1.395(12)
N(2)-C(11)	1.389(12)
N(2)-C(12)	1.393(12)
N(3)-C(14)	1.367(12)
N(3)-C(13)	1.383(12)
C(1)-C(20)	1.472(14)
C(1)-C(2)	1.483(14)
C(1)-C(4)	1.556(13)
C(3)-C(4)	1.539(15)
C(4)-C(5)	1.509(13)
C(5)-C(12)	1.352(13)
C(5)-C(6)	1.418(13)
C(6)-C(7)	1.409(14)
C(6)-C(11)	1.436(14)
C(7)-C(8)	1.365(14)
C(8)-C(9)	1.431(15)
C(9)-C(10)	1.368(14)
C(10)-C(11)	1.380(14)
C(12)-C(13)	1.415(12)
C(13)-C(20)	1.394(13)
C(14)-C(15)	1.364(14)
C(14)-C(19)	1.411(13)
C(15)-C(16)	1.376(14)
C(16)-C(17)	1.413(14)
C(17)-C(18)	1.344(13)
C(18)-C(19)	1.425(13)
C(19)-C(20)	1.446(14)
Cl(3)-C(29)	1.744(9)
Cl(4)-C(37)	1.751(11)
O(5)-C(21)	1.446(11)
O(6)-C(22)	1.220(12)
O(7)-C(23)	1.199(13)
O(8)-C(24)	1.427(12)
N(4)-C(22)	1.370(13)
N(4)-C(23)	1.376(13)
N(5)-C(31)	1.356(12)
N(5)-C(32)	1.379(11)
N(6)-C(33)	1.356(11)
N(6)-C(34)	1.398(12)
C(21)-C(40)	1.502(13)
C(21)-C(22)	1.510(15)
C(21)-C(24)	1.558(14)
C(23)-C(24)	1.564(15)
C(24)-C(25)	1.522(13)
C(25)-C(32)	1.369(13)
C(25)-C(26)	1.400(13)
C(26)-C(31)	1.416(13)
C(26)-C(27)	1.425(13)
C(27)-C(28)	1.401(13)
C(28)-C(29)	1.408(13)
C(29)-C(30)	1.345(13)
C(30)-C(31)	1.393(14)
C(32)-C(33)	1.430(13)
C(33)-C(40)	1.365(13)
C(34)-C(35)	1.390(13)
C(34)-C(39)	1.421(13)
C(35)-C(36)	1.349(13)
C(36)-C(37)	1.421(14)
C(37)-C(38)	1.351(14)
C(38)-C(39)	1.415(13)
C(39)-C(40)	1.420(13)
O(2S)-C(4S)	1.461(13)
C(4S)-C(3S)	1.521(16)
O(1S)-C(1S)	1.423(14)
C(2S)-C(1S)	1.443(17)
C(3)-N(1)-C(2)	112.8(9)
C(11)-N(2)-C(12)	107.3(8)
C(14)-N(3)-C(13)	109.3(8)
O(1)-C(1)-C(20)	107.6(7)
O(1)-C(1)-C(2)	111.6(8)
C(20)-C(1)-C(2)	108.6(9)
O(1)-C(1)-C(4)	111.1(8)
C(20)-C(1)-C(4)	114.0(8)
C(2)-C(1)-C(4)	104.0(8)
O(2)-C(2)-N(1)	122.9(10)
O(2)-C(2)-C(1)	129.5(10)
N(1)-C(2)-C(1)	107.6(9)
O(3)-C(3)-N(1)	123.9(10)
O(3)-C(3)-C(4)	128.2(9)
N(1)-C(3)-C(4)	107.8(10)
O(4)-C(4)-C(5)	113.5(8)
O(4)-C(4)-C(3)	104.3(7)
C(5)-C(4)-C(3)	112.2(9)
O(4)-C(4)-C(1)	109.5(8)
C(5)-C(4)-C(1)	114.7(8)
C(3)-C(4)-C(1)	101.6(8)
C(12)-C(5)-C(6)	108.7(9)
C(12)-C(5)-C(4)	121.5(9)
C(6)-C(5)-C(4)	129.6(9)
C(7)-C(6)-C(5)	137.4(10)
C(7)-C(6)-C(11)	117.0(10)
C(5)-C(6)-C(11)	105.5(9)
C(8)-C(7)-C(6)	120.9(11)
C(7)-C(8)-C(9)	119.7(10)
C(10)-C(9)-C(8)	121.9(10)
C(10)-C(9)-Cl(1)	120.7(9)
C(8)-C(9)-Cl(1)	117.4(8)
C(9)-C(10)-C(11)	117.6(10)
C(10)-C(11)-N(2)	128.8(10)
C(10)-C(11)-C(6)	123.0(10)

N(2)-C(11)-C(6)	108.3(8)	C(25)-C(24)-C(23)	107.5(8)
C(5)-C(12)-N(2)	110.2(9)	C(21)-C(24)-C(23)	102.8(9)
C(5)-C(12)-C(13)	121.2(9)	C(32)-C(25)-C(26)	107.6(9)
N(2)-C(12)-C(13)	128.6(9)	C(32)-C(25)-C(24)	120.7(9)
N(3)-C(13)-C(20)	109.4(9)	C(26)-C(25)-C(24)	131.7(9)
N(3)-C(13)-C(12)	128.6(9)	C(25)-C(26)-C(31)	107.2(9)
C(20)-C(13)-C(12)	121.9(9)	C(25)-C(26)-C(27)	135.9(10)
C(15)-C(14)-N(3)	129.3(10)	C(31)-C(26)-C(27)	116.9(9)
C(15)-C(14)-C(19)	122.5(10)	C(28)-C(27)-C(26)	119.7(9)
N(3)-C(14)-C(19)	108.1(9)	C(27)-C(28)-C(29)	118.8(9)
C(14)-C(15)-C(16)	119.7(10)	C(30)-C(29)-C(28)	123.8(9)
C(15)-C(16)-C(17)	118.2(10)	C(30)-C(29)-Cl(3)	121.3(8)
C(18)-C(17)-C(16)	123.6(10)	C(28)-C(29)-Cl(3)	114.9(8)
C(18)-C(17)-Cl(2)	119.6(9)	C(29)-C(30)-C(31)	117.0(9)
C(16)-C(17)-Cl(2)	116.7(9)	N(5)-C(31)-C(30)	129.3(9)
C(17)-C(18)-C(19)	118.4(9)	N(5)-C(31)-C(26)	107.0(8)
C(14)-C(19)-C(18)	117.6(9)	C(30)-C(31)-C(26)	123.6(9)
C(14)-C(19)-C(20)	107.3(9)	C(25)-C(32)-N(5)	108.3(9)
C(18)-C(19)-C(20)	135.1(10)	C(25)-C(32)-C(33)	122.2(9)
C(13)-C(20)-C(19)	105.8(9)	N(5)-C(32)-C(33)	129.4(9)
C(13)-C(20)-C(1)	121.2(9)	N(6)-C(33)-C(40)	109.7(9)
C(19)-C(20)-C(1)	132.9(9)	N(6)-C(33)-C(32)	129.5(9)
C(22)-N(4)-C(23)	115.1(10)	C(40)-C(33)-C(32)	120.8(9)
C(31)-N(5)-C(32)	109.7(8)	C(35)-C(34)-N(6)	129.7(9)
C(33)-N(6)-C(34)	108.8(8)	C(35)-C(34)-C(39)	123.0(9)
O(5)-C(21)-C(40)	113.0(8)	N(6)-C(34)-C(39)	107.2(8)
O(5)-C(21)-C(22)	104.3(8)	C(36)-C(35)-C(34)	119.0(10)
C(40)-C(21)-C(22)	115.2(9)	C(35)-C(36)-C(37)	118.7(9)
O(5)-C(21)-C(24)	106.7(8)	C(38)-C(37)-C(36)	123.8(10)
C(40)-C(21)-C(24)	113.7(8)	C(38)-C(37)-Cl(4)	118.6(9)
C(22)-C(21)-C(24)	102.9(8)	C(36)-C(37)-Cl(4)	117.6(8)
O(6)-C(22)-N(4)	125.9(11)	C(37)-C(38)-C(39)	118.6(10)
O(6)-C(22)-C(21)	125.6(10)	C(38)-C(39)-C(40)	137.2(10)
N(4)-C(22)-C(21)	108.5(10)	C(38)-C(39)-C(34)	116.9(9)
O(7)-C(23)-N(4)	124.9(11)	C(40)-C(39)-C(34)	105.9(8)
O(7)-C(23)-C(24)	130.4(12)	C(33)-C(40)-C(39)	108.3(9)
N(4)-C(23)-C(24)	104.6(10)	C(33)-C(40)-C(21)	121.7(9)
O(8)-C(24)-C(25)	108.3(8)	C(39)-C(40)-C(21)	129.7(9)
O(8)-C(24)-C(21)	116.2(8)	O(2S)-C(4S)-C(3S)	114.2(10)
C(25)-C(24)-C(21)	113.0(8)	O(1S)-C(1S)-C(2S)	111.2(11)
O(8)-C(24)-C(23)	108.5(8)		

Symmetry transformations used to generate equivalent atoms:

Table S12. Anisotropic displacement parameters ($Å^2$ x 10^3).

The anisotropic displacement factor exponent takes the form: $-2\pi^2[h^2 a^{*2}U11 + ... + 2 h k a^* b^* U12]$

	U^{11}	U^{22}	U^{33}	U^{23}	U^{13}	U^{12}
Cl(1)	62(2)	40(2)	57(2)	-22(2)	23(2)	-8(2)
Cl(2)	85(2)	37(2)	34(2)	-7(1)	16(2)	-11(2)
O(1)	30(5)	49(5)	59(6)	18(4)	-7(4)	-11(4)
O(2)	84(6)	39(5)	19(5)	-2(4)	8(4)	-19(4)
O(3)	47(5)	50(5)	39(5)	-5(4)	13(4)	-5(5)
O(4)	51(5)	32(4)	19(4)	2(3)	4(3)	-7(4)
N(1)	35(6)	40(6)	32(6)	0(5)	15(4)	2(5)
N(2)	37(5)	37(6)	29(6)	-3(5)	6(4)	11(5)
N(3)	17(5)	34(5)	15(5)	5(4)	1(3)	8(4)
C(1)	38(7)	27(6)	24(7)	-8(5)	11(5)	-6(5)
C(2)	50(8)	37(7)	24(7)	14(6)	7(6)	-3(6)
C(3)	56(9)	36(7)	17(7)	1(5)	7(6)	-4(6)
C(4)	40(7)	29(6)	17(7)	12(5)	15(5)	0(5)
C(5)	38(7)	26(6)	18(7)	-5(5)	-3(5)	-1(6)
C(6)	53(8)	42(8)	23(7)	-3(6)	11(5)	13(6)
C(7)	48(7)	31(7)	41(8)	2(6)	13(6)	-11(6)
C(8)	70(8)	29(7)	29(8)	-1(5)	1(6)	0(6)
C(9)	22(6)	27(6)	58(9)	-18(6)	8(5)	4(5)
C(10)	43(7)	39(7)	36(7)	-3(6)	11(5)	1(6)
C(11)	26(6)	33(7)	34(8)	-5(6)	2(5)	-5(5)
C(12)	28(6)	25(6)	12(6)	1(5)	6(4)	1(5)
C(13)	26(6)	44(8)	24(7)	5(6)	1(5)	7(6)
C(14)	22(6)	38(7)	32(7)	-5(6)	8(5)	-3(5)
C(15)	63(8)	42(8)	12(6)	12(6)	9(5)	-5(6)
C(16)	56(8)	52(8)	25(7)	6(6)	12(5)	0(7)
C(17)	36(7)	35(7)	35(7)	-13(6)	20(5)	-10(6)
C(18)	33(6)	38(7)	25(7)	3(6)	-2(5)	7(6)
C(19)	19(6)	42(8)	21(7)	2(5)	11(4)	3(5)
C(20)	21(6)	32(6)	28(7)	-6(5)	8(5)	0(5)
Cl(3)	61(2)	38(2)	31(2)	6(1)	7(1)	-1(2)
Cl(4)	74(2)	34(2)	44(2)	10(1)	8(1)	-4(2)
O(5)	75(5)	25(4)	11(4)	10(3)	1(3)	2(4)
O(6)	56(5)	50(5)	34(5)	4(4)	13(4)	1(5)
O(7)	97(7)	41(5)	17(5)	-4(4)	1(4)	-18(5)
O(8)	53(5)	47(5)	38(5)	-1(3)	-3(4)	5(4)
N(4)	91(9)	37(6)	10(5)	-10(4)	16(5)	1(6)
N(5)	60(6)	27(6)	8(5)	5(4)	10(4)	2(5)
N(6)	27(5)	40(6)	13(5)	-2(4)	2(4)	-9(4)
C(21)	42(7)	31(7)	22(7)	4(5)	5(5)	5(6)
C(22)	46(8)	38(8)	27(7)	27(6)	9(6)	0(7)
C(23)	62(9)	35(7)	28(8)	17(6)	11(6)	-7(7)
C(24)	50(8)	43(7)	13(6)	3(5)	5(5)	22(6)
C(25)	43(7)	21(6)	13(6)	6(5)	19(5)	8(5)
C(26)	28(6)	43(8)	18(7)	-9(5)	7(5)	4(6)
C(27)	61(8)	47(7)	12(6)	-3(6)	10(5)	-6(6)
C(28)	53(8)	32(8)	45(8)	2(6)	8(6)	6(6)
C(29)	49(7)	20(6)	17(6)	13(5)	7(5)	5(5)
C(30)	54(7)	41(8)	14(6)	3(6)	-1(5)	0(6)
C(31)	42(7)	35(7)	9(6)	-3(5)	10(5)	7(5)
C(32)	35(6)	36(7)	5(6)	-2(5)	6(4)	-3(5)

C(33)	31(6)	30(7)	19(7)	-7(5)	-4(5)	7(5)
C(34)	34(7)	27(7)	29(8)	5(5)	1(5)	-1(5)
C(35)	21(6)	48(8)	24(7)	7(6)	6(5)	-1(6)
C(36)	30(7)	24(7)	39(8)	-5(5)	13(5)	4(5)
C(37)	42(7)	32(7)	41(8)	-5(6)	6(6)	3(6)
C(38)	35(7)	39(7)	23(7)	14(6)	6(5)	11(6)
C(39)	17(6)	43(8)	26(7)	1(5)	11(4)	5(5)
C(40)	31(6)	27(6)	23(7)	0(5)	9(5)	-5(5)
O(1W)	56(5)	55(5)	23(4)	-5(3)	2(4)	-5(4)
O(2S)	79(6)	69(6)	53(6)	-17(4)	24(5)	-4(5)
C(4S)	80(10)	40(8)	57(10)	-8(6)	0(7)	22(7)
O(2W)	69(6)	60(5)	22(5)	-19(4)	16(4)	-1(4)
O(1S)	79(6)	61(6)	75(7)	-26(5)	9(5)	-7(5)
C(2S)	81(10)	80(10)	69(10)	23(9)	5(8)	-2(9)
C(3S)	55(8)	101(12)	58(10)	9(8)	-4(7)	10(8)
C(1S)	104(13)	92(13)	54(11)	-3(9)	-2(9)	21(11)

Table S13. Hydrogen coordinates (x 10^4) and isotropic displacement parameters (Å^2 x 10^3).

	x	y	z	U(eq)
H(1A)	11741	7790	10462	70
H(4A)	8497	6485	10903	51
H(1B)	5588	7767	11661	42
H(2A)	7340	6973	5924	41
H(3A)	7969	7930	6126	26
H(7A)	7055	5917	9852	47
H(8A)	6179	5239	8675	51
H(10A)	6304	6021	5479	47
H(15A)	8557	8897	5985	46
H(16A)	9445	9584	7173	52
H(18A)	9979	8769	10304	39
H(5B)	1618	7617	3525	56
H(8B)	-1675	6731	4544	70
H(4B)	4418	6310	2790	54
H(5A)	2152	6116	8248	37
H(6A)	2851	7080	8484	32
H(27A)	26	5360	4010	47
H(28A)	-143	4584	4920	52
H(30A)	1501	5137	8326	44
H(35A)	3795	8041	8996	37
H(36A)	4241	8782	8057	37
H(38A)	2993	8187	4640	38
H(2SA)	3025	8157	11596	99
H(4SA)	5394	8790	12825	71
H(4SB)	3183	8930	12512	71
H(1SA)	6982	6026	2721	108
H(23A)	4739	4784	1915	115
H(23B)	4950	5167	826	115
H(23C)	3478	5270	1842	115
H(3SA)	5028	9270	11028	108
H(3SB)	3562	8883	10369	108
H(3SC)	5776	8742	10684	108
H(1SB)	6007	5335	3348	101
H(1SC)	7483	5231	2334	101
H(2WA)	7038	7674	4073	100
H(1WA)	3231	6423	10271	10
H(2WB)	7450	8111	4717	10
H(1WB)	2344	5921	10131	104

Table S14: Gene annotation table for the Lzr gene cluster (GenBank No. KR052816).

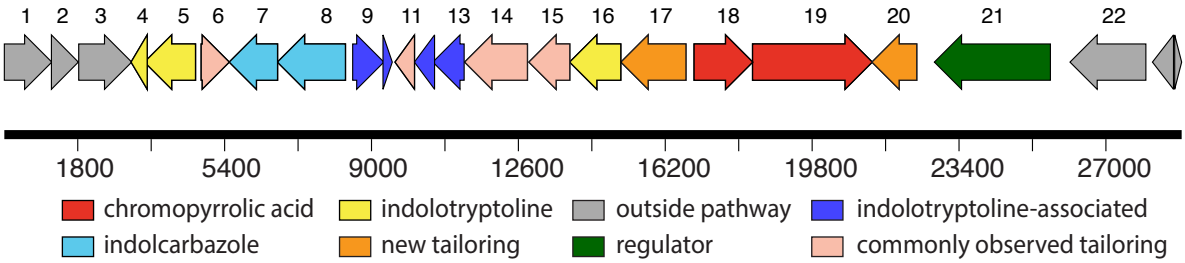

N	Gene	Size (aa)	Homolog	ID/SM	Origin	GenBank Accession
1	*orf -3*	387	Hypothetical protein	80/87	*Lechevalieria aerocolonigenes*	WP_030467181
2	*orf -2*	219	Transcriptional regulator	94/96	*Lentzea albidocapillata*	WP_030481608
3	*orf -1*	432	Beta lactamase	74/81	*Allokutzneria albata*	WP_030429414
4	*lzrX1a*	131	monooxygenase	64/73	Uncultured bacterium AB1650	AEF32090
5	*lzrX1b*	416	monooxygenase	71/78	Uncultured bacterium AB1650	AEF32090
6	*lzrM1*	230	N-methyltransferase	84/93	Uncultured bacterium AB1650	AEF32091
7	*lzrP*	394	RebP-like cytochrome P450	71/80	Uncultured bacterium AB1650	AEF32101
8	*lzrC*	555	RebC-like monooxygenease	80/86	Uncultured bacterium AB1650	AEF32100
9	*lzrY1*	254	Putative alpha/beta hydrolase	65/73	Uncultured bacterium AB1650	AEF32098
10	*lzrY2*	75	Putative alpha/beta hydrolase	58/68	Uncultured bacterium AB1650	AEF32098
11	*lzrF*	159	Putative flavin reductase	71/79	Uncultured bacterium AB1650	AEF32097
12	*lzrT1*	164	Putative cation/H+ antiporter	73/84	Uncultured bacterium AB1650	AEF32096
13	*lzrT2*	255	Putative cation/H+ antiporter	74/85	Uncultured bacterium AB1650	AEF32096
14	*lzrH1*	512	Tryptophan-5 halogenase	85/91	Uncultured bacterium AB1650	AEF32095
15	*lzrM3*	333	O-methyltransferase	73/83	Uncultured bacterium AB1650	AEF32094
16	*lzrX2*	417	monooxygenase	80/87	Uncultured bacterium AB1650	AEF32093
17	*lzrH2*	530	Tryptophan-6 halogenase	79/88	*Lechevalieria aerocolonigenes*	WP_030469177
18	*lzrO*	478	RebO-like L-amino acid oxidase	71/81	Uncultured bacterium	AHE14860
17	*lzrD*	977	RebD-like chromopyrrolic acid synthase	74/83	Uncultured bacterium	AHE14873
18	*lzrG*	365	Cytochrome P450	46/64	*Amcolatopsis decaplania*	WP_007032990
19	*lzrR*	947	LuxR-like transcription regulator	56/70	Uncultured bacterium AB1650	AEF32102
20	*orf+1*	619	Putative PA domain-containing protein	43/58	*Streptomyces viridochromo-genes*	WP_003999481
21	*orf+2*	171	Hypothetical protein	82/91	*Catelliglobosispora koreensis*	WP_020522983
22	*orf+3*	56	peptidase	41/66	*Lentzea albidocapillata*	WP_030482217